The cellular response capacity (CRC) as a novel immunomonitoring approach in sepsis

David Alexander Christian Messerer, Paul Müller, Lisa Wohlgemuth, Frederik Münnich, Laura Stukan, Adam Omar Khalaf Mohamed, Jürgen Benjamin Hagemann, Alexander Sebastian Koller, Darko Jovanovski, Simon Lauer, Rebecca Traut, Leonard Schöbel, Bertram Dietrich Thomaß, Finn Münnich, Eberhard Barth, Manfred Weiss, Andreas Liebold, Bettina Jungwirth, Markus Huber-Lang

Angaben zur Veröffentlichung / Publication details:

Messerer, David Alexander Christian, Paul Müller, Lisa Wohlgemuth, Frederik Münnich, Laura Stukan, Adam Omar Khalaf Mohamed, Jürgen Benjamin Hagemann, et al. 2026. "The cellular response capacity (CRC) as a novel immunomonitoring approach in sepsis." *Military Medical Research* 13 (1): 100010. https://doi.org/10.1016/j.mmr.2026.100010.

Messerer *et al. Mil Med Res* 2026
https://doi.org/10.1016/j.mmr.2026.100010

MMR MILITARY MEDICAL RESEARCH

RESEARCH Open Access

The cellular response capacity (CRC) as a novel immunomonitoring approach in sepsis

David Alexander Christian Messerer[1*], Paul Müller[1], Lisa Wohlgemuth[1], Frederik Münnich[1], Laura Stukan[1], Adam Omar Khalaf Mohamed[1], Jürgen Benjamin Hagemann[2], Alexander Sebastian Koller[3], Darko Jovanovski[4], Simon Lauer[1], Rebecca Traut[1], Leonard Schöbel[1], Bertram Dietrich Thomaß[1], Finn Münnich[1], Eberhard Barth[5], Manfred Weiss[6], Andreas Liebold[4], Bettina Jungwirth[5] and Markus Huber-Lang[1]

Abstract

Background: Early recognition of sepsis remains difficult in clinical practice because conventional humoral biomarkers such as C-reactive protein, procalcitonin, and interleukin-6 (IL-6) exhibit unfavorable, slow-release kinetics and rise hours after the onset of infection. Flow cytometry enables upstream, cell-based immunomonitoring, but its clinical use is restricted by poor standardization of fluorescence measurements. In this study, the neutrophil cellular response capacity (CRC) was developed and evaluated as a standardized approach for rapid assessment of systemic inflammation in bacteremia and sepsis.

Methods: The CRC is based on a flow cytometry-based framework that defines a stable maximal stimulation reference point for neutrophil granulocytes. The CRC was evaluated in a human *ex vivo* whole blood bacteremia model with graded exposure to *Escherichia coli* and compared with humoral inflammatory markers. Next, the CRC was assessed in a prospective intensive care unit sepsis cohort. Moreover, preliminary validation was performed in an independent sepsis cohort and in patients undergoing cardiac surgery.

Results: In the bacteremia model, the CRC of neutrophil markers CD10, CD11b, and CD66b increased in a dose-dependent manner with increasing bacterial burden and detected inflammation at lower pathogen burdens than IL-6 and other humoral mediators, with a superior area under the receiver operating characteristic curve. In clinical sepsis, the CRC discriminated patients from age- and sex-matched healthy volunteers, with the CRC of CD11b showing the highest diagnostic performance. CRC values increased over time in patients with sepsis, consistent with immunological recovery. The maximal stimulation reference point for CD11b remained stable across inflammatory states, cohorts, and instruments. In addition, the CRC more precisely captured the onset and resolution of surgery-induced inflammation than conventional biomarkers.

Conclusions: The CRC provides a rapid, standardized, and robust cell-based immunomonitoring tool that outperforms traditional humoral markers in experimental bacteremia and reliably identifies sepsis in clinical cohorts, strongly supporting its use as a novel biomarker for earlier, more precise sepsis diagnosis and monitoring.

Key words Sepsis, Bacteremia, Immunomonitoring, Neutrophil granulocytes, Flow cytometry, *Escherichia coli* (*E. coli*)

Background

Sepsis is a life-threatening disease [1] that poses a major clinical and scientific challenge in both civilian and military settings [2,3]. Globally, sepsis affects approximately 50 million individuals each year and accounts for approximately 11 million deaths [4]. Combat-related severe tissue trauma, blast injuries, and burns are frequently associated with high rates of local and systemic infections and with the development of early and late sepsis [3-7]. Sepsis is characterized by a dysregulated host response to infection, often resulting in immune dysfunction, shock, multiple organ dysfunction syndrome (MODS), and death [1]. Since delays in appropriate antimicrobial therapy substantially increase mortality in septic shock, diagnostic tools that enable earlier recognition of sepsis and timely initiation of treatment are essential for improving patient outcomes [8,9].

The most common cause and primary driver of sepsis is bacterial infection, accompanied by corresponding pathogen-associated molecular patterns (PAMPs) [10,11]. Conserved molecular structures on bacterial surfaces, such as lipopolysaccharide (LPS) and lipoteichoic acid, function

*Correspondence: David Alexander Christian Messerer, david.messerer@uni-ulm.de
[1]Institute of Clinical and Experimental Trauma Immunology, University Hospital Ulm, 89081 Ulm, Germany
Full list of author information is available at the end of the article

Received: 18 August 2025 Accepted: 05 March 2026

as PAMPs that activate both the humoral and cellular components of the innate immune system [12]. Neutrophils are pivotal in the first line of cellular defense against pathogens sensed via PAMPs and in the response to damage-associated molecular patterns (DAMPs) [13-15]. However, in sepsis, the dysregulated immune response can lead to excessive and uncontrolled neutrophil activation, resulting in overwhelming inflammation and collateral damage to host tissues [13].

To complement the Sepsis-3 criteria, which require clinical evidence of organ dysfunction, numerous biomarkers have been proposed [16-18] to support sepsis diagnosis, monitor disease progression, and differentiate sepsis from sterile systemic inflammation [19]. Humoral biomarkers are synthesized by (immune)cells involved in sensing, transducing, and translating danger signals associated with emerging infection [12]. However, established biomarkers such as C-reactive protein (CRP), procalcitonin (PCT), and interleukin (IL)-6, typically rise 4–12 h after the onset of infection and peak between 1–3 d [20,21], which substantially limits their diagnostic utility. This delay is particularly problematic in both civilian and military emergency settings. Moreover, current diagnostic approaches often lack the sensitivity and specificity needed for the early recognition of sepsis [9,14,21].

In contrast to these downstream humoral biomarkers, cellular biomarkers, which can be readily detected by flow cytometry, represent a more upstream readout of immune activation, enabling rapid detection of surface marker changes triggered by PAMPs or DAMPs. For example, flow cytometry-based analyses can improve the identification, subtyping, and disease severity stratification of severe sepsis [17,22-24]. Given their high prevalence among leukocytes, rapid appearance, and short lifespan, neutrophil expression patterns and associated functional changes may offer more timely and sensitive detection of microbial challenges [25,26]. For example, a meta-analysis based on Sepsis-2 criteria demonstrated that neutrophil Fcγ-receptor (CD64) expression outperformed CRP and PCT in diagnosing sepsis [27]. Although flow cytometry is a powerful tool, its application in emergency clinical settings remains limited due to challenges in standardizing fluorescence intensity measurements [26].

To address these limitations, the cellular response capacity (CRC) method was developed as a robust and widely accessible immunomonitoring approach designed for the rapid detection and monitoring of pathogen-related inflammation. The CRC quantifies neutrophil activation potential by comparing defined marker expression under unstimulated conditions with maximal *in vitro* stimulation. In this context, neutrophil activation profiles in response to various PAMPs and DAMPs have previously been characterized [28-31].

In this clinical proof-of-concept study, the CRC was developed and evaluated as a standardized flow cytometry-based immunomonitoring approach in an *ex vivo* bacteremia model and in patients with sepsis. Specifically, the present study investigated whether a maximal *in vitro* stimulation point for defined neutrophil marker profiles provides a stable reference independent of prior cellular activation, and compared the diagnostic performance and timeliness of CRC-based immunomonitoring with traditional sepsis indicators in settings relevant to both civilian and military care.

Methods

Whole blood model

All experiments were conducted in accordance with the ethical standards of the Declaration of Helsinki and were approved by the Local Independent Ethics Committee of the Ulm University (#319/20). Blood was drawn after written informed consent had been obtained. The setup of the human whole blood model has previously been described [30] and applied [28,29]. In the present study, whole blood was collected into standard neutral monovettes (Sarstedt, Nümbrecht, Germany) supplemented with 0.5 IU heparin per ml. Subsequently, the monovettes were exposed to either phosphate-buffered saline (PBS) with calcium and magnesium ($PBS^{+/+}$, #14080055, Gibco, Thermo Fisher Scientific, Waltham, USA) and the bacterial culture media [buffer control of *Escherichia coli* (*E. coli*) suspension, hereafter referred to as BuC], viable *E. coli* bacteria (ATCC line 25922, DSMZ, Braunschweig, Germany), or LPS (100 ng/ml, from *E. coli* O55:B5, #L2637, Sigma Aldrich, Steinheim, Germany). *E. coli* was employed at final concentrations of 2000, 5000, 10 000, 20 000, and 50 000 colony-forming units (CFU) per ml. An additional sample was directly processed for flow cytometry and had no contact with the model (depicted as "0^{-}").

After sampling, 9 ml of blood was transferred to 33-cm-long heparin-coated tubes (Cortiva, #M999413C, Medtronic, Meerbusch, Germany). The tube ends were affixed to a circuit via a similarly coated connector (Cortiva, #CB4629, Medtronic, Ireland). An air bubble of approximately 1.5 ml was retained within the system to facilitate a continuous blood circulation. The loops were attached to a rotating wheel (Snijders Labs, Tilburg, Netherlands) operating at 7 rpm. The system was then incubated for a period of 60 min at a temperature of 37 °C. Subsequently, the loops were cut open. Initially, 95 μl of blood was drawn directly into dry heparin-anticoagulated glass capillary tubes for subsequent blood

gas analysis (ABL 800 Flex, Radiometer GmbH, Krefeld, Germany). The remaining blood was immediately transferred into citrate-anticoagulated monovettes (Sarstedt, Nümbrecht, Germany) for the analysis of all other parameters.

Samples from patients with sepsis, validation cohorts, and healthy volunteers (HV)

All experiments were conducted in accordance with the Declaration of Helsinki and approved by the Local Independent Ethics Committee of the Ulm University (#319/20). Written informed consent was obtained from all patients before participation. In cases where patients were unable to provide consent at the time of admission, temporary consent was obtained from the next of kin. Definitive consent or refusal was subsequently obtained from the patient or their legal representative. The 14 patients of the sepsis cohort were recruited at the perioperative (non-cardiac surgery) intensive care unit (ICU) of the Clinic for Anesthesiology and Intensive Care Medicine of Ulm University Hospital. The inclusion criteria were as follows: the ability to provide written informed consent, age ≥18 years, admission to the ICU, and sepsis as defined by the current consensus definition [a new increase in Sequential Organ Failure Assessment (SOFA) score of ≥2 and suspected infection within the previous 12 h] [1]. For patient recruitment, a modified SOFA score that excluded the neurological component (Glasgow Coma Scale) was calculated to avoid artificial score changes due to sedation or mechanical ventilation. The exclusion criteria were: active malignant disease with ongoing radiotherapy, chemotherapy, or immunomodulatory treatment, or a life expectancy of less than 24 h. Blood samples were collected within 12 h post-diagnosis (labeled "0"), and subsequently at 24, 72, and 120 h (±10%). Sex- and age-matched (±5 years) HV served as the control group.

For preliminary validation of the findings from the initial sepsis cohort, two additional patient cohorts were included: 8 patients with sepsis (hereafter referred to as sepsis_validation) and 8 patients undergoing cardiac surgery (hereafter referred to as cardiac_surgery_validation).

The sepsis_validation cohort was approved under the same ethics protocol and adhered to the same inclusion and exclusion criteria as the initial sepsis cohort described above. Eight additional patients with sepsis were enrolled, and sex- and age-matched (±5 years) HV served as the control group.

The cardiac_surgery_validation cohort was established after ethical approval (#452/21, Local Independent Ethics Committee of the Ulm University). Written informed consent had been obtained before enrollment. The cohort represents a follow-up study of a recently published patient group [32]. The 8 patients of the cardiac_surgery_validation cohort were recruited at the Clinic for Cardiothoracic and Vascular Surgery, University Hospital Ulm. After surgery, the patients were transferred to the perioperative (cardiac surgery) ICU of the Clinic for Anesthesiology and Intensive Care Medicine of Ulm University Hospital. Inclusion criteria comprised the ability to provide written informed consent, age ≥18 years, and planned surgical aortic valve replacement with extracorporeal circulation. Exclusion criteria included revision procedures, active malignant disease with ongoing radiotherapy or chemotherapy, and current immunomodulatory medication. Blood samples were collected at admission (AD; typically the day before surgery), during surgery [operating room (OR); 45 min after initiation of extracorporeal circulation], and at 24 h and 120 h after the end of surgery (±10%). The cardiac_surgery_validation cohort was also analyzed at the AD time point as the preoperative baseline.

All experimental procedures were identical across the initial sepsis cohort and both validation cohorts (sepsis_validation and cardiac_surgery_validation). The validation cohorts were analyzed using the same flow cytometer and reagents (albeit with different reagent batches), although the instrument had undergone major hardware updates, including laser replacement. It is noteworthy that in patients with sepsis, the exact timing of pathogen translocation and subsequent organ injury is difficult to determine; the onset and duration of the inflammatory stimulus can be precisely defined in surgical settings. Therefore, the main purpose of the sepsis_validation cohort was to validate technical consistency and reproducibility. The cardiac_surgery_validation cohort was used to assess the inflammatory kinetics, specifically to evaluate the kinetics of the changes in cellular and humoral inflammation.

In all cohorts, samples were obtained via peripheral venipuncture or from peripheral arterial or central venous catheters and were collected in citrate-anticoagulated monovettes (Sarstedt, Nümbrecht, Germany). Blood samples from patients or HV were always processed within a similar time frame. All samples were processed within 1 h. This study [30] and another study [33] have demonstrated that neutrophil surface marker expression remains stable during this period.

Markers of humoral inflammation

For the samples of the *ex vivo* whole blood model, the plasma concentrations of matrix metallopeptidase 9 (MMP9, #DY911, R&D Systems, Minneapolis, USA), IL-6 (#555220,

BD Biosciences, San Jose, USA), and IL-8 (#DY208, R&D Systems) were measured in citrate-anticoagulated plasma using enzyme-linked immunosorbent assay according to the respective manufacturer's instructions.

For all samples from the patient cohorts, myeloperoxidase (MPO), MMP9, serum amyloid A (SAA), and calprotectin (also known as MRP8-14) were quantified using a LEGENDplex Human Vascular Inflammation Panel 1-S/P (#740809, Biolegend, San Diego, USA) in accordance with the manufacturer's instructions.

Hematological analysis and markers of humoral inflammation

Sodium, potassium, ionized calcium, and glucose were measured using a standard blood gas analyzer (ABL 800 Flex, Radiometer GmbH, Krefeld, Germany). Differential blood count was determined using a standard hematology analyzer (Sysmex CN 2000, Sysmex, Kobe, Japan), according to the respective manufacturer's standard protocol. CRP was measured by a turbidimetric assay on a cobas c system (Roche, Penzberg, Germany). PCT was quantified by an electrochemiluminescence immunoassay on a cobas 8000/e 801 system (Roche, Penzberg, Germany). Creatinine and bilirubin were measured by a photometric assay on a cobas c system (Roche, Penzberg, Germany). All the above-listed parameters were analyzed in cooperation with the Department of Clinical Chemistry of the University Hospital Ulm.

The CRC

This study applied the CRC to samples from an *ex vivo* whole blood model of bacteremia and to samples from patients with clinical sepsis or surgery-related inflammation as described above. Three distinct methodological approaches for the CRC, each with a unique set of features (e.g., requirement for a centrifugation step, turnaround time, and data yield), are summarized in Fig. 1 and Additional file 1: Table S1 and described below.

The classic CRC

For the analysis of neutrophil phenotype, a total of 5 μl of citrate-anticoagulated blood was incubated with a cocktail of 10 μmol/L N-formylmethionyl-leucyl-phenylalanine (fMLF, #F3506, Sigma-Aldrich, Steinheim, Germany), 1 μmol/L platelet-activating factor (PAF, #18779, Cayman Chemical Company, Ann Arbor, Michigan, USA), and 2.3 nmol/L tumor necrosis factor (TNF, 210-TA-005/CF, R&D Systems), or PBS without calcium and magnesium ($PBS^{-/-}$, #14190250, Gibco, Thermo Fisher Scientific) as buffer control. Next, staining was performed with antibodies (all from BioLegend, if not indicated otherwise, San Diego, California, USA) against CD10 [Phycoerythrin-Cyanine 7 tandem fluorochrome (PE-Cy7), 0.6 μg/ml, #312214; isotype #400126], CD11b [Allophycocyanin (APC) fluorochrome, 0.3 μg/ml, #101212; isotype #400612], CD15 [Fluorescein isothiocyanate (FITC), 1.0 μg/ml, #301904; isotype #401606], CD16 [Peridinin-chlorophyll-protein complex fluorochrome (Per-CP), 0.5 μg/ml, #302030; isotype #400148], and CD62L [R-phycoerythrin fluorochrome (PE), 2.5 μg/ml, #304806; isotype #400112]. The samples were brought up to a total volume of 50 μl by adding ($PBS^{-/-}$) and were incubated for 15 min in a light-protected water bath at 37 °C.

The stained and stimulated blood was transferred to 950 μl of BD FACS Lysing Solution (#349202, BD Biosciences, USA) and incubated for 30 min at room temperature in the dark. Following centrifugation at 340×*g* for 5 min, the supernatant was discarded, and the cells were resuspended in 100 μl $PBS^{-/-}$ but containing 1% bovine serum albumin (BSA, A8022, Sigma Aldrich, USA). Finally, the samples were stored at 4 °C in the dark until measurement, which was typically performed within 60 min.

For all experiments, a minimum of 3000 granulocytes were recorded using a BD FACSLyric (BD Biosciences, USA) or a BD FACSCanto II (BD Biosciences, USA). For the FACSLyric, intra-instrument variability was corrected daily by the standard quality check using CS&T-Beads of BD. The gating strategy is summarized in Additional file 1: Fig. S1. Representative raw data are provided in Additional file 2. Doublets were excluded by plotting forward scatter (FSC) area vs. height and assessing the linearity of these parameters. Granulocytes were identified based on their FSC and side scatter (SSC) area characteristics. Among granulocytes, neutrophil granulocytes constitute the most abundant cell type. Because the analysis was conducted using the median fluorescence intensity (MFI), small intra-individual deviations of the neutrophil percentage within the granulocyte fraction had no relevant influence on the MFI. Although small proportions of basophils and eosinophils are present within the granulocyte population, the use of the median justified referring to the analyzed cells as neutrophil granulocytes throughout this work. Spectral spillover between fluorescence channels was corrected using a compensation matrix (Additional file 3). For all antigens, appropriate isotype and single-stain controls were included (data not shown).

The simple CRC

A total of 9 μl of citrate-anticoagulated blood was incubated with an antibody mix supplemented with $PBS^{-/-}$ up to a total volume of 50 μl at 37 °C in a water bath for 10 min. The

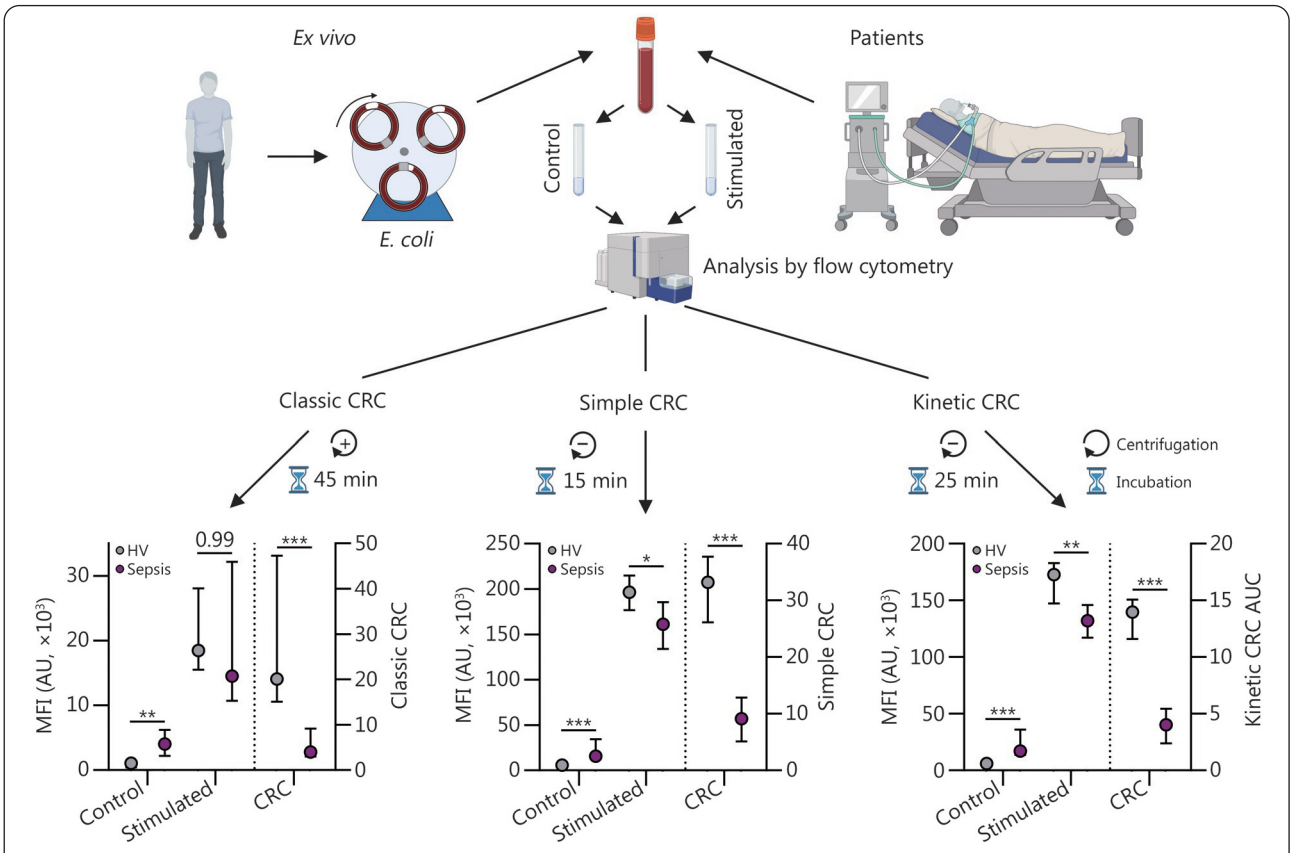

Fig. 1 Methodological workflow from sample preparation to measuring the cellular response capacity (CRC).
Following blood collection, samples are prepared for flow cytometric analysis either unstimulated (PBS as buffer control) or stimulated with an inflammatory cocktail (cocktail of N-formylmethionyl-leucyl-phenylalanine, platelet-activating factor, and tumor necrosis factor). The CRC is calculated as the ratio of median fluorescence intensity (MFI) between stimulated and unstimulated neutrophils. Three approaches, classic, simple, and kinetic CRC, offer distinct advantages and limitations based on technical aspects such as manual processing steps (e.g., centrifugation) and incubation time. n=13–14. Statistical analysis was performed using the Kruskal-Wallis test with Dunn's post-hoc test, comparing patients with sepsis at all time points (shown in the figure: 0 h, not shown in the figure: 24, 72, 120 h) with healthy volunteers (HV). P-values are indicated above the respective data points. Asterisks indicate significant differences between HV and patients at 0 h only. *P<0.05, **P<0.01, ***P<0.001. AUC. Area under the curve; AU. Arbitrary units; PBS. Phosphate-buffered saline; *E. coli*. *Escherichia coli*

antibody mix contained CD10 (PE-Cy7, 8 μg/ml, #312214; isotype #400126), CD11b (APC, 8 μg/ml, #101212; isotype #400612), CD16 (Per-CP, 16 μg/ml, #302030; isotype #400148), CD35 (FITC, 8 μg/ml, #332406; isotype #400108), CD45 (Pacific blue, 4 μg/ml, #368540), and CD62L (PE, 1 μg/ml, #304806; isotype #400112), CD66b [Allophycocyanin-Cyanine 7 tandem fluorochrome (APC-Cy7), 8 μg/ml, #305126]. Subsequently, the blood was carefully transferred into tubes prefilled with 1550 μl of $PBS^{+/+}$ and incubated at 37 °C in a water bath for another 2 min.

Following incubation, the cells were measured using a BD FACSLyric flow cytometer. During the measurement, the respective test tube was held at a body temperature of 37 °C by a syringe heater (Warner Instruments, Holliston, USA) connected to a temperature control unit (Warner Instruments, Holliston, USA). After the measurement, a stimulation cocktail consisting of fMLF, PAF, and TNF in 200 μl $PBS^{+/+}$ was added, which, after addition, resulted in a final concentration of 10 μmol/L fMLF, 1 μmol/L PAF, and 2.3 nmol/L TNF.

For the simple CRC, at least 600 neutrophils were measured, and gating was performed as summarized in Additional file 1: Fig. S2. Representative raw data are provided in Additional file 2. The top 1 to 2 percent of CD45-positive cells (Pacific blue) were first selected by setting a threshold to reduce the number of cells to process. Doublets were removed by plotting the FSC area vs. the height, followed by analyzing the linearity of both parameters. Subsequently, the remaining cells were stratified by their SSC area and CD16 (PerCP) fluorescence intensity before isolating the neutrophils by applying a CD45 (Pacific blue) vs. CD66b (APC-Cy7) gate. The spillover between the fluorescence channels was corrected by a compensation matrix (Additional file 3). For all antigens,

appropriate isotype controls and single-stain controls were performed (data not shown).

The kinetic CRC

The kinetic CRC was measured as described before [34]. In total, 9 μl (samples from patients with sepsis) or 20 μl (samples from the *ex vivo* whole blood model) citrate-anticoagulated blood was diluted and supplemented with $PBS^{-/-}$ accumulating to a total volume of 50 μl containing the following antibodies (all from BioLegend): CD11b (final concentration: 8 μg/ml), CD35 (8 μg/ml), CD10 (8 μg/ml), CD16 (16 μg/ml), CD62L (1 μg/ml), CD45 (Pacific blue, 4 μg/ml), and CD66b (APC-Cy7, 8 μg/ml). Cells were stained in a light-protected water bath at 37 °C for 10 min. The stained blood was transferred into a 5 ml polystyrene round-bottom tube with a total volume of 1550 μl $PBS^{+/+}$. Before the transfer, the tube was perforated at a height of 4.5 cm using a soldering station (BASETech, Hirschau, Germany), forming a small hole with a diameter of approximately 7–10 mm. Following a resting period of 2 min in the water bath at 37 °C, the sample was placed in the manual acquisition port of the BD FACSLyric flow cytometer. The tube was surrounded by a temperature-controlled heating unit (#TC-124A Handheld Temperature Controller, 64-1545, Warner Instruments, Holliston, MA, USA) set to 37.3 °C. Acquisition at medium speed was started and continued for 1320 s. After 55 s, a peripheral venous catheter (Vasofix Safety 1.30×45 mm G 18, #4268130S-01, B. Braun, Melsungen, Germany) was placed in the polystyrene tube during the acquisition. Attached to the peripheral venous catheter was a 1 ml syringe (BD Plastipak, #303172, Becton Dickinson S.A. Madrid, Spain) containing 150 μl stimulation mixture. Following a 60 s baseline measurement, the content of the syringe was rapidly injected into the polystyrene tube, followed by a bolus of 200–300 μl air to ensure the proper mixing of the stimulants. The stimulation mixture consisted of fMLF, PAF, and TNF in 200 μl $PBS^{+/+}$, which, after injection, resulted in a final concentration of 10 μmol/L fMLF, 1 μmol/L PAF, and 2.3 μnmol/L TNF.

The gating strategy was identical to that described for the simple CRC (Additional file 1: Fig. S2). Based on this gating strategy, a median of 21.6 (13.2–31.7) neutrophils per second in patients with sepsis and a median of 11.8 (10.0–13.7) neutrophils per second in HV was measured. The identified neutrophils were further analyzed using a custom-written flow cytometry analytics software "BFlow" (BFlow Project, www.bflow.science). For this purpose, a moving median of 9 consecutive neutrophils was calculated for each parameter. To analyze the resulting kinetics, the response of the neutrophils was divided into three parts (seconds in brackets refer to the total acquisition time with neutrophils being stimulated after 60 s): baseline (10–50 s), initial stimulation (60–90 s), and response kinetics (90–960 s). A representative illustration is shown in Fig. 2. For curve approximation, the measurement continued with a total measurement period of 1320 s. The baseline was defined as the median of the measurement within 10–50 s. The response kinetics was fit as a polynomial of the 5th order. The polynomial was fitted using the moving median of 65–1140 s. However, because it is difficult to distinguish effects induced by either fMLF, PAF, and TNF from those caused by mixing of the cells, directly after stimulation, the 60–90 s (first 30 s after stimulation) were approximated by a linear curve starting from the baseline and ending at the polynomial-derived value of 90 s. Examples of the resulting fits are summarized in Fig. 2.

For the evaluation and analysis of the kinetic CRC, the baseline was determined as described above. Subsequently, changes after stimulation were normalized to this baseline, and the resulting curves were integrated over time to calculate the area under the curve (AUC). This process is summarized with the equation: $\int_{60}^{960} \frac{f(x)}{baseline} dx$, where x denotes seconds after initiation of the measurement.

Statistical analysis

The flow cytometry data, including neutrophils, monocytes, and platelets, were analyzed using custom-written, Python-based flow cytometry analysis software "BFlow" (BFlow Project, www.bflow.science, last accessed 31 October 2025). Data analysis was performed with Microsoft Excel 2019 (Microsoft, Redmond, USA) and GraphPad Prism 10 (GraphPad Software Inc., San Diego, USA). All data were presented as the median with error bars indicating the interquartile range (IQR). In the manuscript, data are reported as median (IQR). Figure 1 was partially created using Biorender.com.

The CRC was calculated as the ratio of the median MFI of neutrophils from blood samples stimulated with an inflammatory cocktail by their corresponding buffer control, with the formula of $CRC = \frac{MF1\ stimulated}{MF1\ unstimulated}$. Receiver operating characteristic (ROC) curves were calculated using the Wilson/Brown method. AUC values of the ROC curves are reported with the 95% confidence interval (95% CI). To calculate the half-maximal effective concentration (EC_{50}), data were normalized to buffer control (Ctrl)=0% (bottom) and LPS 100 ng/ml=100% (top). The Ctrl was included in the EC_{50} calculation as two logarithmic steps below the lowest *E. coli* concentration. EC_{50} was calculated

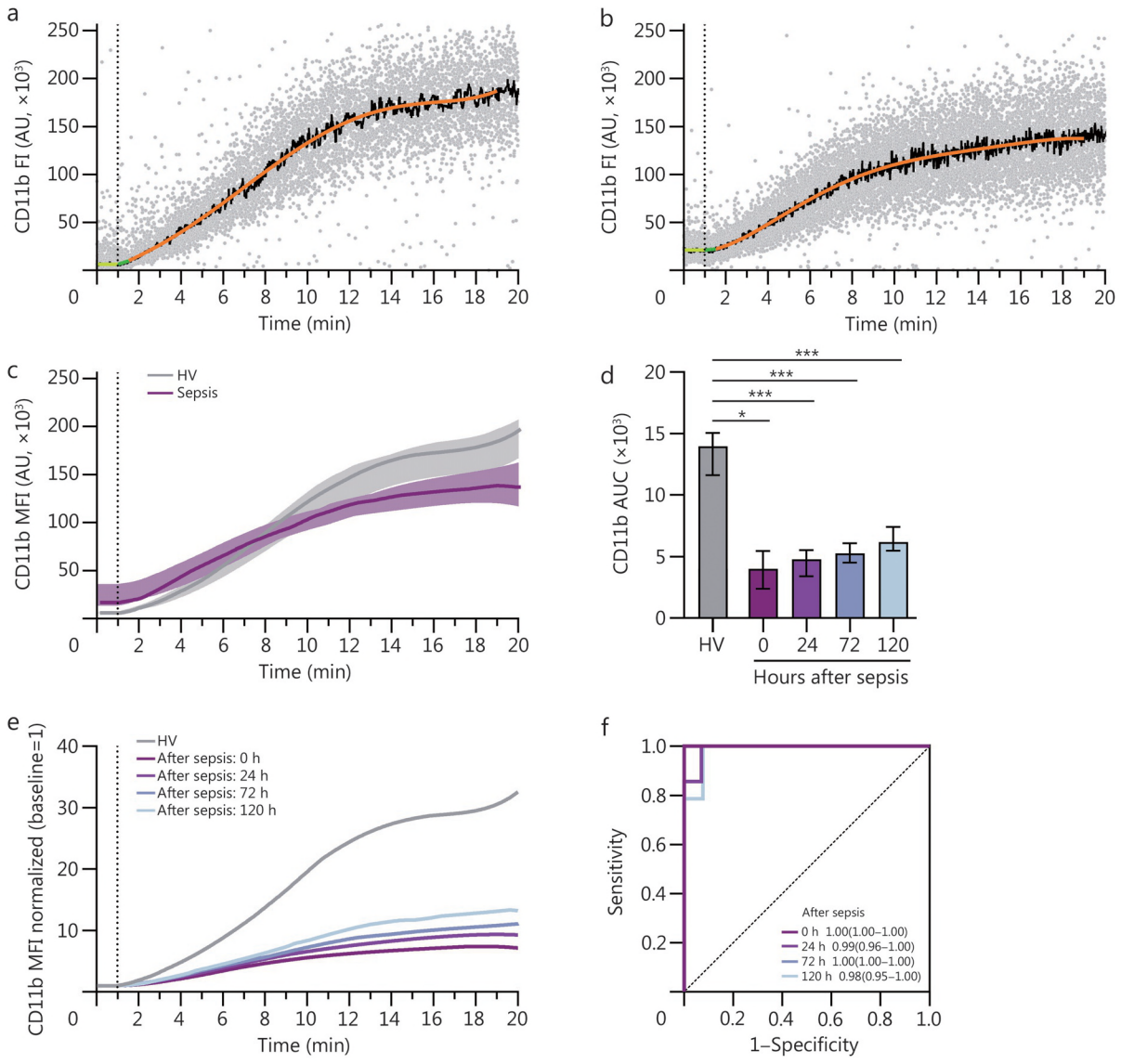

Fig. 2 The kinetics of CD11b expression as an activity marker of neutrophil granulocytes during sepsis.

Fluorescence intensity (FI) in arbitrary units (AU) of neutrophil granulocytes from the representative healthy volunteer (HV, **a**) and from the representative patient with sepsis (**b**) at the time of diagnosis over 20 min after stimulation (vertical dotted line) with a cocktail of N-formylmethionyl-leucyl-phenylalanine, platelet-activating factor, and tumor necrosis factor (n=1). In both cases, the plots report single cells (gray points), the resulting moving median with a window of 45 cells (black line), and a polynomial function (orange line) with baseline (yellow line) and connecting straight line (green line) as described in the method section. **c** Polynomial functions of the CD11b expression of neutrophil granulocytes from patients with sepsis at the time of diagnosis (violet line) and HV (gray line) after stimulation [median and (IQR)] (n=14). **d** Area under the curve (AUC) of the polynomial functions of CD11b expression of neutrophil granulocytes from patients with sepsis and HV after stimulation (n=14). **e** Normalized median polynomial functions of CD11b expression of neutrophil granulocytes of patients with sepsis and HV after stimulation (n=14). **f** Receiver operating characteristic (ROC) curves to analyze the performance of the kinetics of CD11b expression of neutrophil granulocytes (n=14). ROC curves were calculated using the Wilson/Brown method. AUC values of the ROC curves are reported with the 95% confidence interval. Values are shown as median with or without IQR. Statistical analysis was performed using the Kruskal-Wallis test with Dunn's post-hoc test, comparing patients with sepsis at all time points (0, 24, 72, 120 h) with HV. P-values are indicated above the respective data points. *P<0.05, ***P<0.001. IQR. Interquartile range; MFI. Median fluorescence intensity

using the formula: $Y=bottom+\frac{top-bottom}{1+10^{(log(EC_{50})-X)*Hillslope}}$, with Y indicating response, X indicating decadic logarithm of the concentration, and *top* and *bottom* indicating plateaus in the units of the Y-axis. For the calculation of a summarized EC_{50} combining multiple donors, the EC_{50} values were calculated combining all the respective experiments in a single fit and were reported as the best-fit value with a 95% CI. To compare

EC_{50}, for example, the EC_{50} value of a marker for neutrophil phenotype (measured as MFI) and the CRC, the EC_{50} value for each donor was calculated and subsequently statistically analyzed. In general, for the comparison of two groups, a two-sided Mann-Whitney *U* test was performed. For the analysis of multiple groups (patients during the course of sepsis), a Kruskal-Wallis test followed by Dunn's post-hoc test was conducted. The performed tests are indicated in the respective figure legends. A *P*-value <0.05 was considered to be significant. Significance is denoted by *, **, and ***, indicating <0.05, <0.01, and <0.001, respectively. *r* indicates the Spearman correlation coefficient. Cohen's *d* was calculated using the formula: $Cohen's\ d = \frac{mean_1 - mean_2}{\sqrt{\frac{SD_1^2 + SD_2^2}{2}}}$, with *SD* indicating standard deviation.

Results

E. coli whole blood model gradually evokes inflammation

The HV for the *ex vivo* whole blood model were between 22 and 32 years old, with 4 male and 4 female donors. The *ex vivo* whole blood model provided a stable environment to simulate conditions of systemic inflammation (Additional file 1: Table S2) as described previously. In brief, contact between blood and the tubing system did not result in significant changes in potassium levels or platelet counts, which would otherwise indicate hemolysis and/or platelet activation. Similarly, blood gas values (partial pressures of oxygen and carbon dioxide) remained relatively stable throughout the analysis period and generally resembled those of venous blood. As expected, there was a moderate decrease in glucose as well as an increase in lactate when comparing 0^- with the other experimental conditions after 60 min (Additional file 1: Table S2). The stability of the model system was also evident in neutrophil activation markers (CD10, CD11b, CD16, and CD62L) and markers of humoral inflammation (IL-6, IL-8, and MMP9) (Additional file 1: Table S3). Consistent with previous observations in a model of endotoxemia [28], bacteremia with viable *E. coli* resulted in a dose-dependent increase in humoral inflammatory markers, specifically IL-6, IL-8, and MMP9 (Fig. 3).

The CRC outperforms standard humoral markers of inflammation in an *ex vivo* model of bacteremia

Based on the experience in previous studies [30,34], 5 selected parameters (CD10, CD11b, CD15, CD16, and CD62L) of neutrophil activation were evaluated in the bacteremia model. Exposure to *E. coli* resulted in a dose-dependent increase in neutrophil activation markers as indicated by differences in CD11b expression and corresponding increases in CD11b ROC-values (Fig. 4). Due to logistical reasons, the classic, the simple, and the kinetic CRC were only compared in the context of endotoxin exposure but not bacteremia. Additional file 1: Fig. S3 illustrates technical aspects of the kinetic CRC. In detail, the addition of PBS as buffer control, as well as control for adding substances in general, including potential physical irritation of neutrophils, did not result in neutrophil activation as indicated by CD11b. Figure 5 reports significant differences in all 3 CRC approaches, illustrating that the classic, the simple, and the kinetic CRC reliably distinguish between blood samples with and without LPS exposure. Figure 6 summarizes the EC_{50} of humoral markers in comparison to the classical CRC. The classic CRC of CD10 (EC_{50}=4056 CFU/ml) and CD11b (EC_{50}=4219 CFU/ml) performed best in comparison to IL-6 (EC_{50}=10 128 CFU/ml).

Clinical characteristics of the sepsis cohort

The findings of the *ex vivo* bacteremia study were further corroborated in patients with clinical sepsis. In summary, 14 sepsis patients with a female-to-male ratio of 6–8 and a median age of 80 (67–83) years, as well as 14 sex- and age-matched HV, were included. Among the patients, 6/14 received steroids at the diagnosis of sepsis (exploratory evaluation of steroid therapy on the CRC, which did not affect the CRC to distinguish patients with sepsis from HV, is reported in Additional file 1: Fig. S4). On the first measurement time point, the patients with sepsis received the following antibiotics, all prior to sampling: 10/14 piperacillin/tazobactam and 4/14 meropenem. In this cohort, 8/14 patients survived over 90 d. The primary suspected origin in the cohort of patients with sepsis was abdominal infection (9/14). On admission, the median SOFA score was 7 (4–9). Further details and kinetics of traditional markers of inflammation, including leukocyte count, neutrophil-lymphocyte ratio, CRP, PCT, IL-6, and IL-8, are reported in Fig. 7 and Additional file 1: Table S4. Because sepsis was already clinically evident, most of those traditional markers, as well as further markers of humoral inflammation such as SAA, calprotectin, MMP9, and MPO, reached their peak on admission and improved during the course of stay in the ICU.

In-depth analysis of potential neutrophil parameters for the CRC

Throughout the present work, a total of 35 neutrophil-related parameters were evaluated by using the classical CRC approach comparing patients with sepsis and HV (Fig. 8; Additional file 1: Figs. S5-S10). Additional file 4 reports the full results of the screening process. Based on the stability of fluorescence values

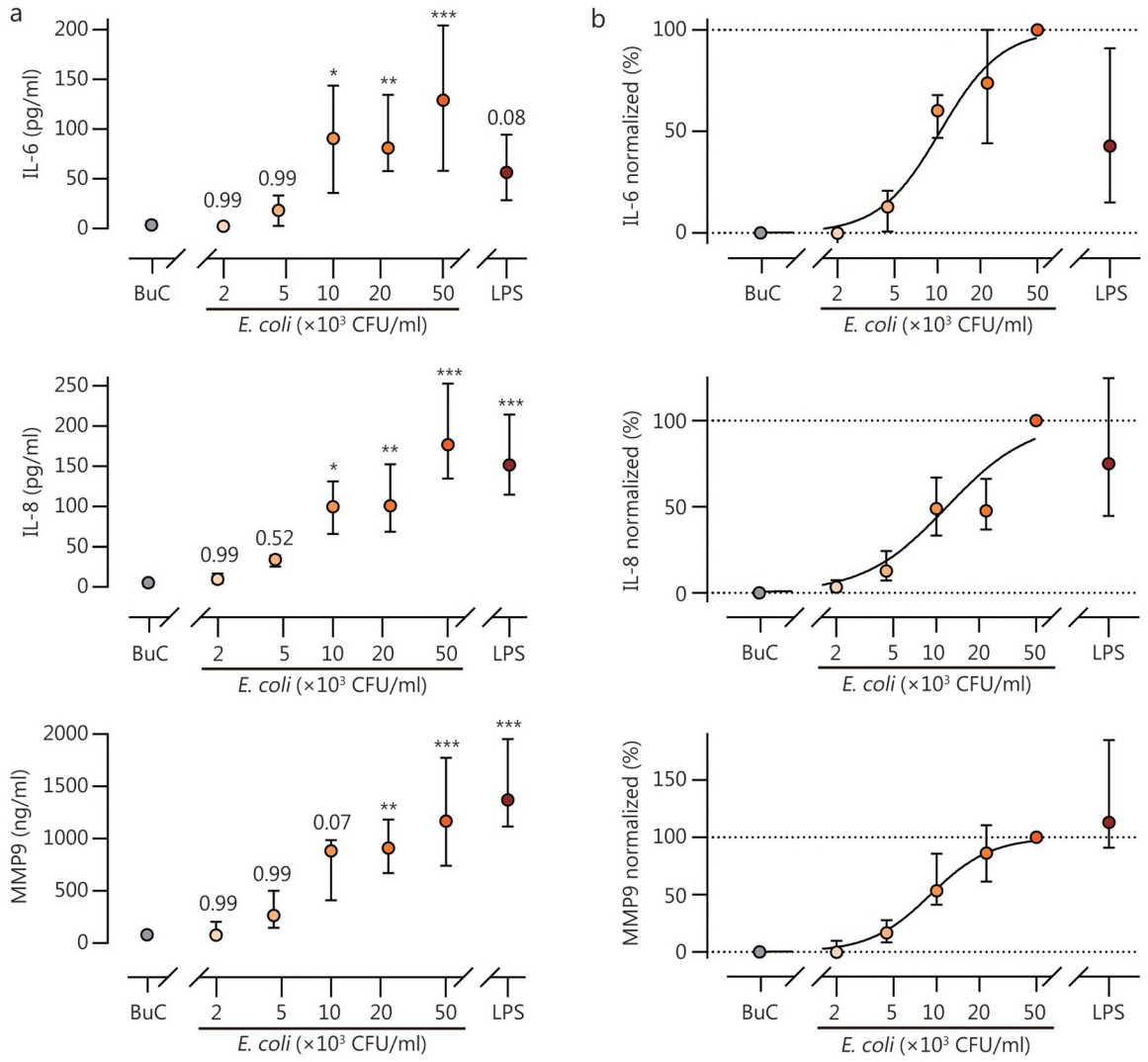

Fig. 3 Concentration-dependent change in the humoral inflammatory response following incubation with *Escherichia coli* (*E. coli*) in the *ex vivo* whole blood model.

a Absolute plasma concentrations of IL-6, IL-8, and MMP9 determined by enzyme-linked immunosorbent assay. **b** Normalized values and EC_{50} curve fit by BuC=0% and 50 000 CFU/ml *E. coli*=100%, respectively, for IL-6, IL-8, and MMP9 as indicated by EC_{50} (%) on the respective Y-axis. BuC indicates buffer control after 60 min incubation; numbers on the X-axis indicate *E. coli* bacteria in concentrations of 2000 to 50 000 CFU/ml after 60 min incubation; LPS indicates lipopolysaccharide (LPS) 100 ng/ml after 60 min incubation. Values are shown as median and interquartile range. n=8. Statistical analysis was performed using the Kruskal-Wallis test with Dunn's post-hoc test, comparing all shown concentrations of *E. coli* bacteria and 100 ng/ml LPS with BuC. P-values are indicated above the respective data points. *P<0.05, **P<0.01, ***P<0.001. CFU. Colony-forming units; IL. Interleukin; MMP9. Matrix metallopeptidase 9

after stimulation over the course of sepsis and effect sizes of stimulated and unstimulated cells, CD10, CD11b, CD66b, and CD62L were subsequently reported, evaluated, and discussed in detail. For all three approaches of the CRC, significant changes were observed comparing patients with sepsis and HV (Figs. 2 and 8). A more detailed analysis revealed that CD10 and CD11b consistently exhibited the highest ROC values and/or the highest effect sizes (Cohen's d) across most comparisons (Additional file 1: Fig. S6). It is noteworthy that the CRC increased during the ICU stay of the patients with sepsis, which might reflect progressive immunological recovery (Figs. 2 and 8). Although the simple and kinetic CRC generally yielded higher ROC values than the classic CRC for most parameters, the observed differences were typically modest and were currently considered unlikely to be of clinical significance (Additional file 1: Fig. S6).

CD11b was identified as the most promising marker and is described in detail across the different CRC measurement approaches (Figs. 2 and 9). Figure 2 provides a detailed overview of the fitting procedure used for the kinetic CRC,

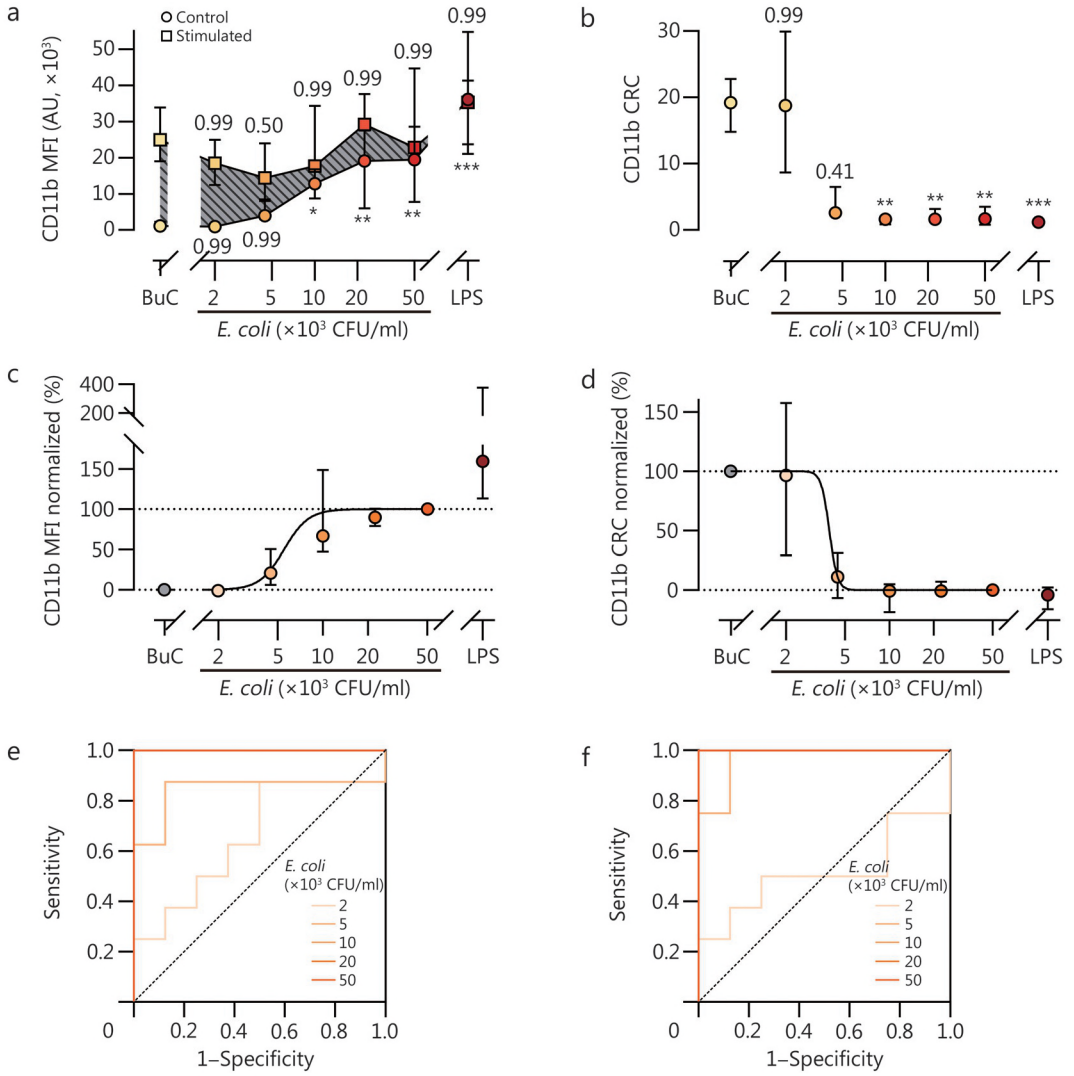

Fig. 4 CD11b as an activity marker of neutrophil granulocytes during bacteremia in the *ex vivo* whole blood model.
a Median fluorescence intensity (MFI) of CD11b unstimulated (Control) and stimulated (cocktail of N-formylmethionyl-leucyl-phenylalanine, platelet-activating factor, and tumor necrosis factor) neutrophil granulocytes. **b** Cellular response capacity (CRC) of CD11b as the ratio of stimulated and unstimulated samples from **a**. **c** Normalized values and EC_{50} curve fit by BuC=0% and 50 000 CFU/ml *Escherichia coli* (*E. coli*)=100% of unstimulated data from **a** as indicated by EC_{50} (%) on the respective Y-axis. **d** Normalized values and EC_{50} curve fit by BuC=100% and 50 000 CFU/ml *E. coli*=0% of the CRC from **b** as indicated by EC_{50} (%) on the respective Y-axis. Receiver operating characteristic curves to analyze the performance of unstimulated CD11b MFIs (**e**) and calculated CRC based on the Wilson/Brown method (**f**). BuC indicates buffer control after 60 min incubation; numbers on the X-axis of **a**-**d** indicate *E. coli* bacteria in concentrations of 2000 to 50 000 CFU/ml after 60 min incubation; LPS indicates lipopolysaccharide (LPS) 100 ng/ml after 60 min incubation. Values are shown as median and interquartile range. n=8. Statistical analysis was performed using the Kruskal-Wallis test with Dunn's post-hoc test, comparing all shown concentrations of *E. coli* bacteria and 100 ng/ml LPS with BuC. P-values are indicated above or below the respective data points. *P<0.05, **P<0.01, ***P<0.001. AU. Arbitrary units; CFU. Colony-forming units

as described in the Methods section. Figure 9 illustrates the analysis of the assumption that there is a cellular reference point of maximal stimulation (after exposure to fMLF, TNF, and PAF) that is reached irrespective of prior stimulation status in both HV and patients with sepsis. This fixed reference point might help standardize CD11b expression, which was significantly increased in patients with sepsis (Fig. 9). The classic, simple, and kinetic CRC all successfully distinguished HV from patients with sepsis.

Preliminary validation

Finally, a preliminary validation of the generalizability of the CRC was performed, taking into account the corresponding limitations and implications discussed in the respective section. To this end, two validation cohorts (sepsis_validation and cardiac_surgery_validation cohorts with different

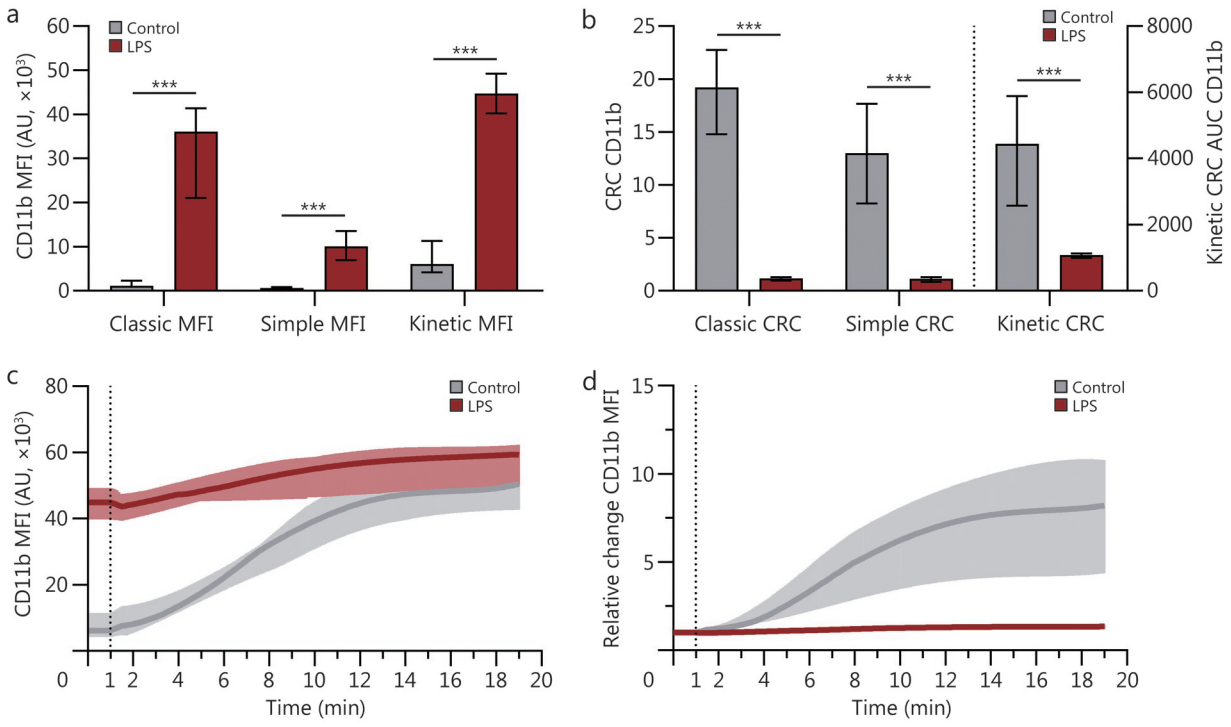

Fig. 5 Comparison of different approaches to measure the cellular response capacity (CRC) for CD11b on neutrophil granulocytes.

Blood from healthy volunteers was incubated with either PBS (Control) or 100 ng/ml LPS for 60 min in the *ex vivo* whole blood model. **a** Analysis of the median fluorescence intensity (MFI). **b** Evaluation of the CRC as determined by different approaches (classic, simple, and kinetic CRC). **c**, **d** Change in fluorescence intensity and change in CRC using the kinetic CRC approach, comparing blood with previous exposure to LPS or PBS (buffer control) from the *ex vivo* whole blood model. In both **c** and **d**, the single-cell values measured by flow cytometry were condensed using a moving median with a window of 9 cells. This moving median was then approximated with a 5th-degree polynomial function. The plots display these polynomial functions together with the baseline (median before stimulation) and a connecting line from the baseline to the polynomial function for 30 s after stimulation. Values are shown as median and interquartile range. n=10. Statistical analysis was performed using the Mann-Whitney U test. ***P<0.001. AU. Arbitrary units; LPS. Lipopolysaccharide; PBS. Phosphate-buffered saline

underlying pathophysiologies and from different ICUs from the same hospital) were included. For both cohorts, traditional inflammatory markers (CRP, IL-6, PCT, leucocytes) are presented in Additional file 1: Fig. S11.

Eight sepsis patients with a female-to-male ratio of 2–6 and a median age of 60 (37–74) years, as well as 8 sex- and age-matched HV, were included. On the first measurement time point, the patients with sepsis received the following antibiotics, all prior to sampling: 5/8 piperacillin/tazobactam and 3/8 meropenem. Despite being measured on a modified instrument setup, as described in the methods section, the CRC, including its fixed reference point, remained stable (Additional file 1: Figs. S12-S15).

The cardiac_surgery_validation cohort comprised patients with a surgically induced inflammatory stimulus. This cohort enabled a more precise evaluation of the CRC with respect to its ability to monitor the kinetics of inflammation. Importantly, in this setting, the exact onset of the acute systemic inflammatory trigger was known. Here, 8 patients undergoing open aortic valve replacement with extracorporeal circulation were included, with a female to male ratio of 0–8 and a median age of 62 (56–70) years. In this cohort, representing DAMP-driven acute systemic inflammation, the fixed reference point of the CRC was confirmed. Furthermore, both the onset and postoperative resolution of inflammation were captured more accurately by the CRC compared with CRP and other humoral markers of inflammation (Additional file 1: Figs. S11-S15).

Last, for the initial sepsis cohort, the inter-device difference of CD11b was analyzed using samples from the same patients stained with the same antibodies. Figure 9 demonstrates that the inter-device comparison resulted in a high comparability between the two measurement setups.

Discussion

Rapid and accurate diagnosis of sepsis remains a clinical challenge and an unmet medical need, primarily due to

a

		CD10	CD11b	CD15	CD16	CD62L	IL-6	IL-8	MMP9
ROC	CRC vs. MFI	CRC	CRC	CRC	CRC	CRC			
	ROC	1.000	1.000	0.688	0.844	1.000	0.891	0.938	0.875
	95% CI	1.000–1.000	1.000–1.000	0.410–0.965	0.610–1.000	1.000–1.000	0.686–1.000	0.809–1.000	0.646–1.000
	P-value	0.0008	0.0008	0.2076	0.0209	0.0003	0.0087	0.0033	0.0117
EC_{50}	CRC vs. MFI	CRC	CRC			MFI			
	EC_{50} (CFU/ml)	4056	4219			1950	10 128	15 776	10 504

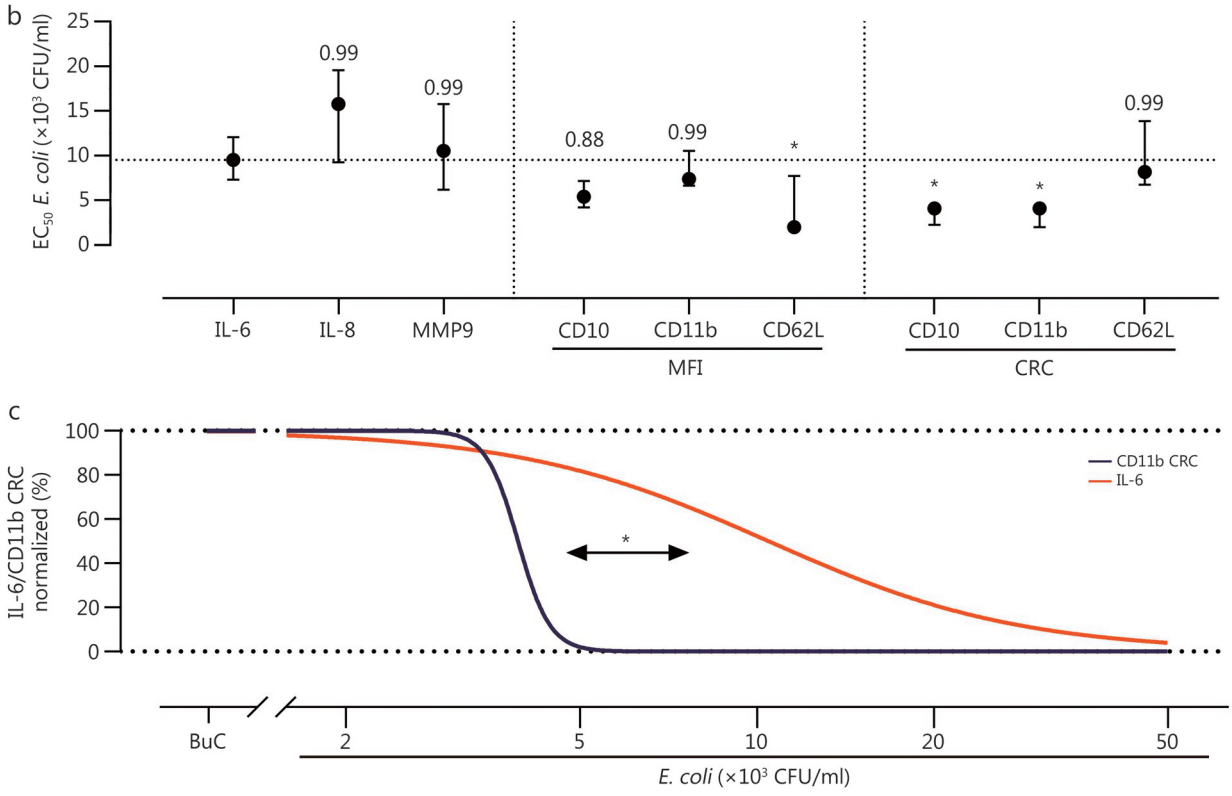

Fig. 6 Diagnostic performance for the detection of bacteremia, analyzing the neutrophil phenotype by determining the median fluorescence intensity (MFI) and the cellular response capacity (CRC) in comparison with traditional markers of humoral inflammation (IL-6, IL-8, MMP9).

a Comparison of receiver operating characteristic (ROC) at 10 000 CFU/ml *Escherichia coli* (*E. coli*) with the respective 95% confidence interval (CI) and *P*-value, and half-maximal effective concentration (EC_{50}) as a function of the *E. coli* concentration. **b** Detailed comparison of the EC_{50} as a function of the *E. coli* concentration. **c** Exemplary comparison of EC_{50} curve fit after normalization as indicated by EC_{50} (%) on the respective Y-axis to BuC=100% and 50 000 CFU/ml *E. coli*=0% for the humoral marker IL-6 (the IL-6 values were multiplied by −1 before EC_{50} calculation to facilitate comparability with the CRC) and the change in neutrophil phenotype represented by CD11b CRC. BuC indicates buffer control after 60 min incubation; numbers on the X-axis of c indicate *E. coli* bacteria in concentrations of 2000 to 50 000 CFU/ml after 60 min incubation. Values are shown as median and interquartile range. n=8. Statistical analysis was performed using the Kruskal-Wallis test with Dunn's post-hoc test, evaluating the EC_{50} of IL-8, MMP9, the MFI, and CRC of CD10, CD11b, and CD62L in comparison to the EC_{50} of IL-6. *P*-values are indicated above the respective data points. *P<0.05. CFU. Colony-forming units; IL. Interleukin; MMP9. Matrix metallopeptidase 9

technical limitations and the absence of reliable target biomarkers with favorable kinetic properties. Utilizing a human whole blood model and a prospective proof-of-concept sepsis study, the present study demonstrates that the CRC of neutrophils, rapidly measurable by flow cytometry, effectively addresses standardization challenges in sepsis diagnostics. Consistent with previous unpublished findings in *ex vivo* endotoxemia models, it was observed that the CRC exhibited reduced sensitivity in detecting bacteremia. The potential diagnostic head start offered by CRC requires

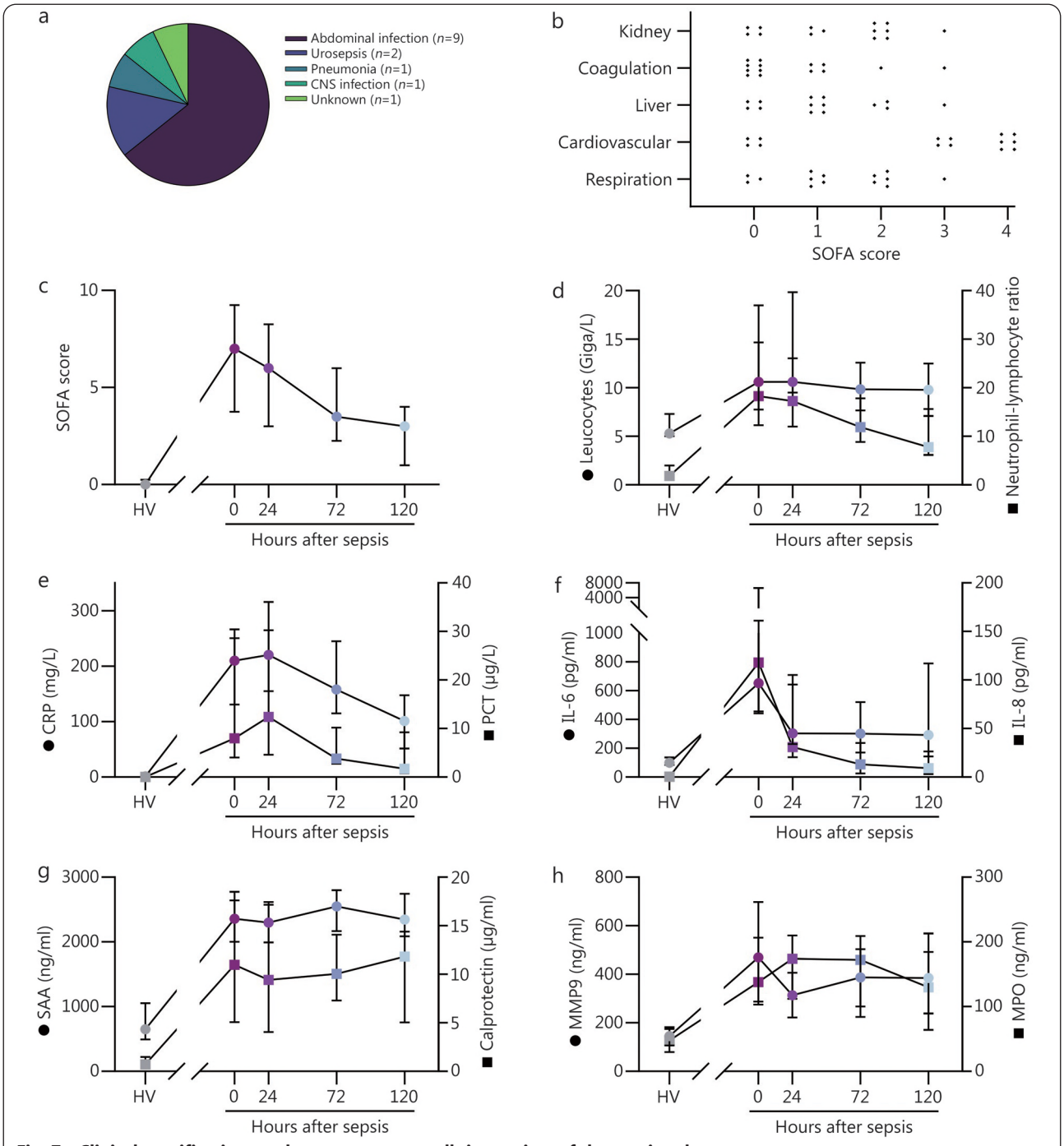

Fig. 7 Clinical specifications and parameters over all time points of the sepsis cohort.

a Suspected infection cause of sepsis. **b** Distribution of the individual score points of the Sequential Organ Failure Assessment (SOFA) score. **c** Total SOFA score. **d**-**h** Traditional and humoral markers of inflammation: leukocytes and neutrophil-lymphocyte ratio (**d**), C-reactive protein (CRP) and procalcitonin (PCT) (**e**), interleukin-6 (IL-6) and interleukin-8 (IL-8) (**f**), serum amyloid A (SAA) and calprotectin (**g**), matrix metallopeptidase 9 (MMP9) and myeloperoxidase (MPO) (**h**). Values are shown as median and interquartile range. *n*=14. CNS. Central nervous system; HV. Healthy volunteers

further validation in clinical settings. However, this effort is complicated by the difficulty in determining the exact onset of pathogen translocation and sepsis development. Nonetheless, the present findings suggest that CRC-based immunomonitoring not only outperforms conventional sepsis markers in terms of sensitivity and specificity but also substantially accelerates the detection of infection and sepsis.

The persistent challenge of delayed sepsis diagnosis is reflected in the current Sepsis-3 diagnostic criteria [1]. These criteria require a suspected or confirmed infection along with

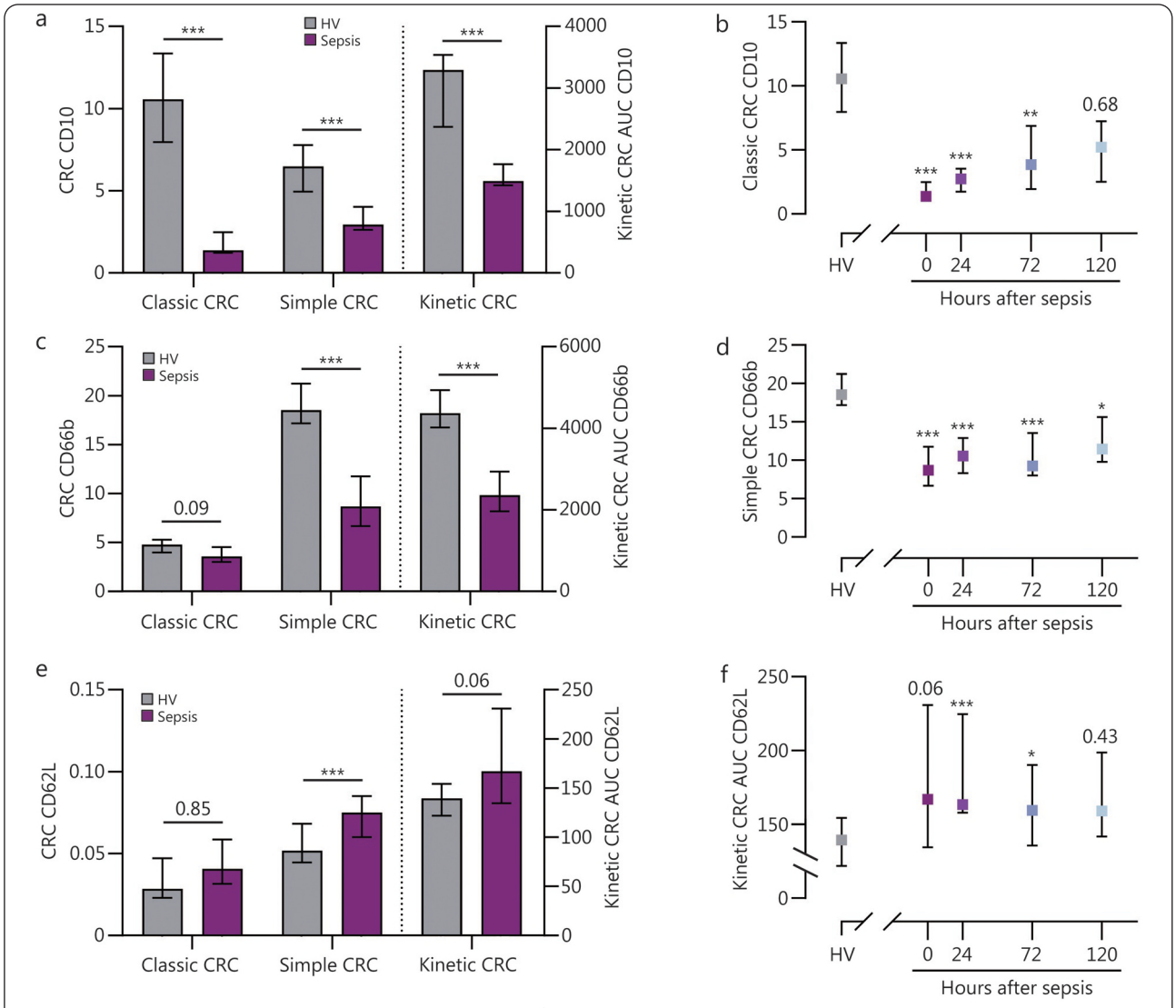

Fig. 8 CD10, CD66b, and CD62L as activity markers of neutrophil granulocytes among patients with sepsis vs. healthy volunteers (HV).

a Comparison of CD10 between the different methods [classic, simple, and kinetic cellular response capacity (CRC)] at the diagnosis time point. **b** CRC of CD10 as the ratio of stimulated and unstimulated cells, calculated with classic CRC. **c** Comparison of CD66b between the different methods (classic, simple, and kinetic CRC) at the diagnosis time point. **d** CRC of CD66b as the ratio of stimulated and unstimulated cells, calculated with simple CRC. **e** Comparison of CD62L between the different methods (classic, simple, and kinetic CRC) at the diagnosis time point. **f** AUC of CD62L calculated with kinetic CRC. Values are shown as median and interquartile range. n=13–14. Statistical analysis was performed using the Kruskal-Wallis test with Dunn's post-hoc test, comparing patients with sepsis at all time points (0, 24, 72, 120 h) with HV. P-values are indicated above the respective data points. *P<0.05, **P<0.01, ***P<0.001. AUC. Area under the curve

a 2-point increase in the SOFA score, which typically indicates that organ dysfunction is already clinically apparent. However, immune function, a key contributor to the development of MODS [12], is notably absent from these criteria. In a recent study, the neutrophil-lymphocyte ratio has been added to the quick SOFA score to improve diagnostic accuracy and prognostic capability [35]. The sensitivity and specificity of the SOFA score for diagnosing sepsis have been evaluated in the study [1], with the Sepsis-3 publication reporting an AUC of the ROC curve of 0.74 for predicting in-hospital mortality among patients with suspected infection outside the ICU.

Efforts to enhance sepsis diagnosis have proposed various biomarkers reflecting diverse pathophysiological mechanisms, including inflammation, endotheliopathy, coagulopathy, complementopathy, vasomotor dysfunction, and organ failure [36]. However, these biomarkers, often located relatively downstream in the pathophysiological cascades, require time to be generated and to reach detectable thresholds [36].

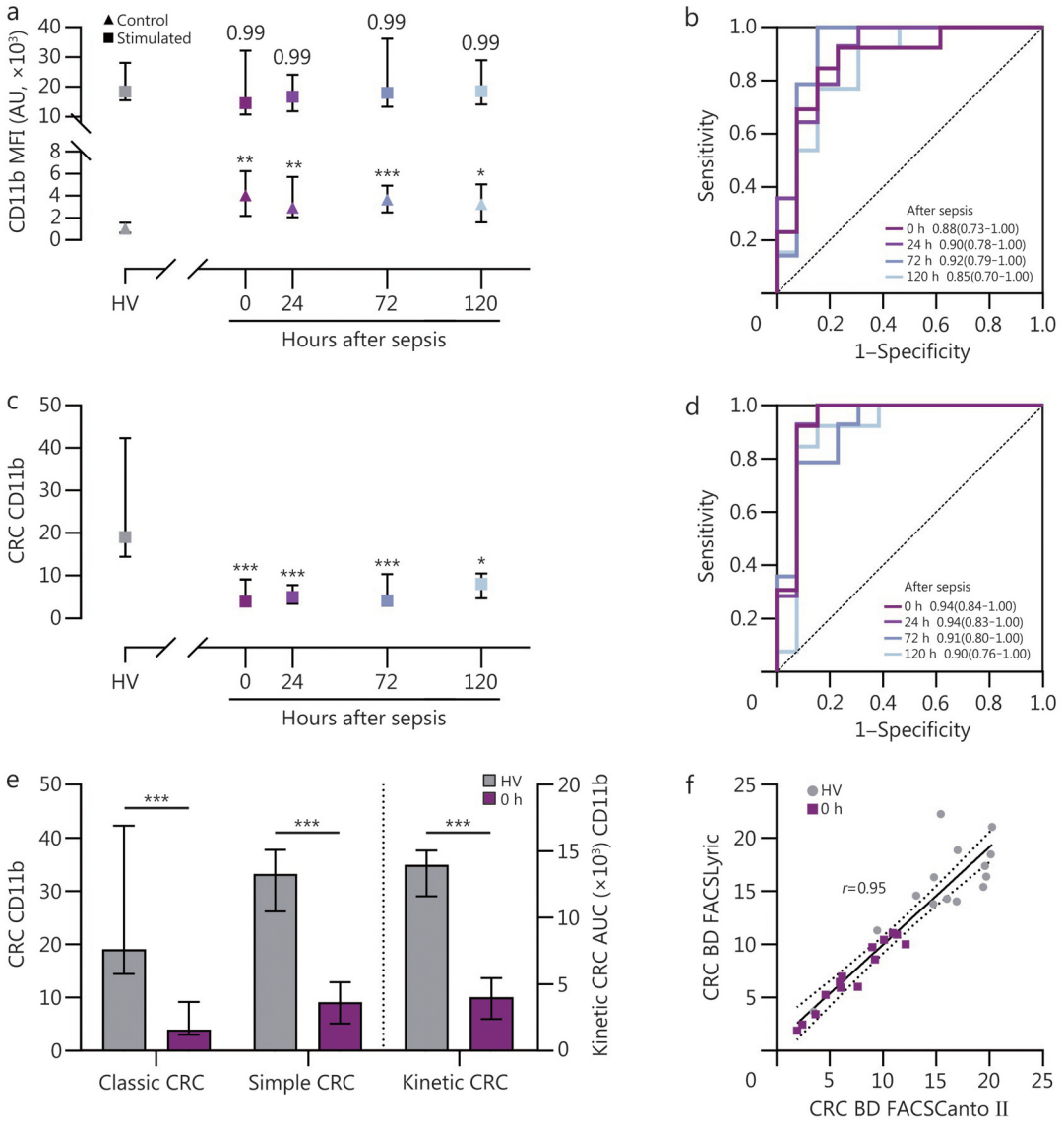

Fig. 9 CD11b as an activity marker of neutrophil granulocytes among patients with sepsis vs. healthy volunteers (HV).
a Median fluorescence intensity (MFI) of CD11b in unstimulated (Control) and stimulated (cocktail of N-formylmethionyl-leucyl-phenylalanine, platelet-activating factor, and tumor necrosis factor) neutrophil granulocytes. **b** Receiver operating characteristic (ROC) curves to analyze the performance of unstimulated CD11b MFI from **a**, area under the curve (AUC) with the 95% confidence interval (95% CI) indicated. **c** Cellular response capacity (CRC) of CD11b as the ratio of stimulated and unstimulated samples from **a**. **d** ROC curves to analyze the performance of the CRC, AUC with the 95% CI indicated. **e** Comparison of the different methods (classic, simple, and kinetic CRC) at the time point of sepsis diagnosis (0 h). **f** Comparison of two different flow cytometers (BD FACSLyric and BD FACSCanto II) for the classic CRC of CD11b. The line represents a simple linear regression with the 95% CI. *r* indicates the Spearman correlation coefficient. Values are shown as median and interquartile range. n=13–14. Statistical analysis was performed using the Kruskal-Wallis test with Dunn's post-hoc test, comparing patients with sepsis at all time points (0, 24, 72, 120 h) with HV. *P*-values are indicated above the respective data points. ROC curves were calculated using the Wilson/Brown method. *P<0.05, **P<0.01, ***P<0.001. AU. Arbitrary units

Consequently, their sensitivity and specificity for rapid and reliable sepsis diagnosis frequently remain suboptimal, with the AUC of the ROC curve often below 0.8 [36]. The combination of clinical assessment and biomarker profiling can improve diagnostic accuracy. For example, incorporating the amount of red blood cells infused within the first 24 h and 4 subsets of lymphocytes and natural killer cells achieved an AUC of 0.89 for severe sepsis diagnosis [22]. Nonetheless, the time elapsed until diagnosis, by which point clinical features have become evident, often remains unacceptably long.

Because neutrophils, the first line of cellular defense, respond rapidly to PAMPs and DAMPs exposure [25,34],

the present work explored their upstream phenotype and function. Initially, an established *ex vivo* human blood model was employed for systematic evaluation of the CRC. The model allows neutrophil phenotype assessment with or without exposure to inflammatory stimuli, without relevant artificial effects from anticoagulants, without additional burden to patients, and without ethical or translational concerns associated with the use of animal models [30]. The pathophysiology of sepsis involves a complex interplay of PAMPs and DAMPs, which perpetuates a vicious cycle of tissue damage, immune dysregulation, thromboinflammation, barrier dysfunction, and the subsequent development of infection, sepsis, and MODS [12]. Clinical evidence suggests that late MODS and mortality in critically ill patients are primarily driven by PAMPs [37]. Consequently, *E. coli* was employed as a source of representative PAMPs, and a standardized mixture of PAMP- and DAMP-containing stimuli was applied as an additional secondary stimulus to drive neutrophils toward the fixed reference point.

Therefore, whole blood samples were subjected to bacteremia simulation with *E. coli*, followed by additional stimulation with a potent PAMP/DAMP/inflammatory mediator cocktail or corresponding buffer control. In a screening process, several markers, including CD10, CD11b, CD16, and CD62L, exhibited immunomonitoring potential, corroborating earlier clinical findings [38]. CD11b, a β2-integrin, functions as the pathogen-sensing complement receptor 3 and a neutrophil activation marker. An advantage of CD11b is its rapid upregulation (within a few minutes) during adhesion and transmigration of neutrophils to the infected site [39], thus covering the very early events in fighting invading microorganisms and PAMPs. In the present model of bacteremia, CD11b on neutrophils was enhanced at concentrations of 10 CFU/μl *E. coli* present and reached a maximal upregulation after additional cocktail stimulation. While *E. coli* increased the CD11b surface expression in a dose-dependent manner, the potential maximal response upon additional stimulation remained approximately the same. This stability enabled the calculation of expression ratios by comparing marker levels under unstimulated and stimulated conditions, termed the CRC. The CRC for CD11b and CD10 markedly outperformed IL-6 in detecting *E. coli* bacteremia in the *ex vivo* whole blood model.

Consistent with the present findings, neonatal sepsis studies reported pooled sensitivity and specificity values with an AUC of 0.90 for CD11b in whole blood [38]. Therefore, the present study advances immunomonitoring using neutrophil markers such as CD11b by introducing a standardized framework based on the CRC in the context of sepsis. This framework relies on the establishment of a fixed reference point that, for certain parameters such as CD11b, remained stable regardless of the presence or absence of sepsis. In the present exploratory data set of sepsis, a confirmation group of patients with sepsis, and patients with coronary artery disease as a comorbidity with or without additional surgery-related acute inflammation, this fixed reference point remained stable irrespective of the inflammatory status. The authors consider this stability the key finding of the current work, as it offers a straightforward means of standardizing setup-specific variables (e.g., instrument type, reagents) to establish normal ranges that can be applied for rapid assessment of a patient's inflammatory status, thereby leveraging the advantages of cell-based over protein-based immunomonitoring. Of note, the present study focused on neutrophils because they are the most abundant circulating leukocytes, characterized by a short lifespan, rapid turnover, and high sensitivity to inflammatory mediators. Nonetheless, further investigations should extend the CRC approach to additional immune cell types, as discussed below.

In a third step, these findings were translated into a simplified CRC approach. This "simple CRC" method involves a 15-minute *ex vivo* incubation without prior centrifugation, enabling a technical turnaround time of less than 30 min. Together with the biological rationale for cell-based rather than protein-based immunomonitoring, as discussed below, such acceleration is potentially advantageous for earlier recognition of sepsis. Earlier and more accurate identification of patients with sepsis, if confirmed in larger translational studies, may facilitate more timely initiation of treatment and thereby improve patient outcomes [8,9]. The near real-time recording of the cellular response with CD11b as a read-out by the kinetic CRC flow cytometry-based method reliably distinguished HV from patients with sepsis within 15–20 min, corresponding to an approximate 30-minute needle-to-diagnosis time. Of note, this rapid lab diagnosis was associated with a notable ROC of 1.00 at the time of clinical sepsis suspicion, and up to 120 h after sepsis diagnosis with an ROC of 0.98. However, these results require cautious interpretation, as the initial evaluation occurred in a small homogenous ICU cohort with evident and already diagnosed clinical sepsis in comparison to age- and sex-matched HV.

Regarding early detection, explicit quantitative comparisons such as AUC or sensitivity beyond the defined time points of the present work were beyond the scope of this exploratory proof-of-concept study. Nevertheless, several complementary findings support the biological plausibility of a faster diagnostic response. First, surface activation markers like CD11b are

preformed and can be rapidly translocated to the neutrophil membrane within minutes, whereas humoral markers such as IL-6 require *de novo* transcription and translation, resulting in delayed release. Second, in the *ex vivo* whole-blood bacteremia model, the CRC parameters increased proportionally with escalating *E. coli* concentrations, demonstrating a graded and rapid cellular response. Third, in the cardiac_surgery_ validation cohort, where the onset of inflammation was precisely defined by surgery and extracorporeal circulation, the CRC captured both initiation and resolution of inflammation with greater temporal precision than conventional biomarkers such as CRP or IL-6.

The differentiation between DAMP- and PAMP-driven inflammation remains to be fully elucidated for the CRC. As previously reported, cellular markers typically precede humoral markers in reflecting inflammatory dynamics [32]. In the present exploratory cohort of cardiac surgery patients, the fixed reference point of stimulated neutrophils remained stable for most CRC parameters even under conditions of surgery and extracorporeal circulation, underscoring the CRC's robustness and its potential applicability to trauma-associated inflammation. Further investigation is warranted to clarify how the CRC behaves in predominantly PAMP- vs. DAMP-driven inflammatory states. Notably, in the present exploratory data set representing DAMP-driven inflammation, CRC-based immunomonitoring exhibited markedly faster kinetics than conventional inflammatory markers. This finding provides a promising foundation for future studies with larger and more heterogeneous cohorts to assess the CRC's clinical utility, for example, for early sepsis recognition at emergency admission and for monitoring subsequent sepsis development. Additionally, as a novel framework for standardizing cellular immunomonitoring, the CRC should be systematically compared with established cellular markers (e.g., CD64) and classical humoral indicators (e.g., leukocyte count, CRP, IL-6). Moreover, future studies will need to elucidate the underlying biological mechanisms that drive parameter differences (e.g., CD11b vs. CD62L).

As a limitation of the present study, the findings are primarily based on a single clone or fluorochrome per surface marker, which may benefit from further optimization. Although inter-device reliability across two flow cytometers was high (r=0.95), variability in instrument settings, reagent variability, antibody quality, and operator expertise remains a concern for broader implementation [40]. Thus, other flow cytometer devices and/or inter-operator variability need to be evaluated, especially for platforms that can be readily implemented in emergency settings. In this context, operability of the CRC under real-world circumstances should be assessed and compared to humoral markers of inflammation and other point-of-care diagnostic approaches. Additionally, while the classical CRC approach with fixation offers flexibility in measurement timing, the kinetic and simple CRC methods prioritize speed but may be more susceptible to technical errors. Overall, the invested time and human resources remain comparable between the methods. Beyond the present exploratory cohort, multicenter studies with larger patient populations that include different causative microbial agents, a broad range of preexisting acute and chronic diseases, and diverse drug regimens (e.g., antimicrobial and immunomodulatory therapies) are essential to further validate CRC in routine clinical practice. Despite these limitations, the method's minimal invasiveness, low blood volume requirement, rapid processing, affordability, and scalability are distinct technical strengths.

For future avenues, further phenotyping of critically ill patients [41] and artificial intelligence-based network analyses may help to investigate, evaluate, and define the optimal combination of clinical, biochemical [42], and functional features for prompt sepsis diagnosis [43]. Moreover, personalized immunotherapy selection following traumatic injuries and/or burns with subsequent risk of sepsis could also benefit from these approaches [44].

Conclusions

Neutrophil granulocytes, as key effector cells of the innate immune system, represent a promising target for cellular immunomonitoring. The CRC of neutrophils enables rapid and reproducible quantification of activation in response to PAMPs, providing a robust framework for standardized, cell-based inflammation assessment. In this proof-of-concept study, the CRC outperformed conventional humoral biomarkers in detecting *ex vivo* bacteremia and reliably discriminated patients with sepsis from HV. Moreover, during sepsis as well as during DAMP-driven inflammation, the newly established fixed reference point included in the CRC remained stable.

With its advantages of speed, sensitivity, minimal invasiveness, and methodological standardization, the CRC offers substantial potential for improving sepsis immunomonitoring and may ultimately contribute to earlier and more precise detection of infection in both civilian and military healthcare settings. Further multicenter validation is warranted to confirm its clinical utility for real-time sepsis diagnosis.

Abbreviations

AD: Admission
APC: Allophycocyanin
APC-Cy7: Allophycocyanin-Cyanine 7 tandem fluorochrome
AU: Arbitrary units
AUC: Area under the curve
BSA: Bovine serum albumin
CFU: Colony-forming units
CRC: Cellular response capacity
CRP: C-reactive protein
DAMPs: Damage-associated molecular patterns
E. coli: *Escherichia coli*
EC_{50}: Half-maximal effective concentration
FITC: Fluorescein isothiocyanate
fMLF: N-formylmethionyl-leucyl-phenylalanine
FSC: Forward scatter
HV: Healthy volunteer
ICU: Intensive care unit
IL: Interleukin
IQR: Interquartile range
LPS: Lipopolysaccharide
MFI: Median fluorescence intensity
MMP: Matrix metallopeptidase
MODS: Multiple organ dysfunction syndrome
MPO: Myeloperoxidase
OR: Operating room
PAF: Platelet-activating factor
PAMPs: Pathogen-associated molecular patterns
PBS: Phosphate-buffered saline
PCT: Procalcitonin
PE: R-phycoerythrin fluorochrome
PE-Cy7: Phycoerythrin-Cyanine 7 tandem fluorochrome
Per-CP: Peridinin-chlorophyll-protein complex fluorochrome
ROC: Receiver operating characteristic
SAA: Serum amyloid A
SOFA: Sequential Organ Failure Assessment
SSC: Side scatter
TNF: Tumor necrosis factor

Supplementary information

The online version contains supplementary material available at https://doi.org/10.1016/j.mmr.2026.100010.

Additional file 1. Fig. S1 Representative flow cytometric gating strategy for assessing classic cellular response capacity (CRC) in neutrophils. **Fig. S2** Representative flow cytometric gating strategy for assessing simple and kinetic cellular response capacity (CRC) in neutrophils. **Fig. S3** Illustration of the difference between control stimulation with phosphate-buffered saline (PBS, as buffer control, horizontal curve) and stimulation cocktail (increasing curve). **Fig. S4** CD11b as activity markers of neutrophil granulocytes of patients with sepsis (*n*=14) at diagnosing time point with differentiation of patients receiving steroids (*n*=6) and patients without steroid treatment (*n*=8). **Fig. S5** Performance analysis of different markers analyzed by median fluorescence intensity (MFI) and the classic cellular response capacity (CRC). **Fig. S6** Performance analysis of different approaches to measure the cellular response capacity (CRC). **Fig. S7** CD62L as an activity marker of neutrophil granulocytes among clinical patients with sepsis vs. healthy volunteers (HV). **Fig. S8** CD64 as an activity marker of neutrophil granulocytes among patients with sepsis vs. healthy volunteers (HV). **Fig. S9** CD279 as an activity marker of neutrophil granulocytes among clinical patients with sepsis vs. healthy volunteers (HV). **Fig. S10** HLA-DR as an activity marker of neutrophil granulocytes among clinical patients with sepsis vs. healthy volunteers (HV). **Fig. S11** Comparison of traditional inflammation markers between the sepsis_validation (Sepsis) and the cardiac_surgery_validation (CS) cohorts. **Fig. S12** Validation of CD10-based immunomonitoring in the sepsis_validation cohort (a, b) and the cardiac_surgery_validation cohort (c, d). **Fig. S13** Validation of CD11b-based immunomonitoring in the sepsis_validation cohort (a, b) and the cardiac_surgery_validation cohort (c, d). **Fig. S14** Validation of CD62L-based immunomonitoring in the sepsis_validation cohort (a, b) and the cardiac_surgery_validation cohort (c, d). **Fig. S15** Validation of CD66b-based immunomonitoring in the sepsis_validation cohort (a, b) and the cardiac_surgery_validation cohort (c, d). **Table S1** Comparison of protocol variants for standardized assessment of classic, simple, and kinetic neutrophil cellular response capacity (CRC). **Table S2** Evaluation of the stability of the whole blood model of bacteremia by blood gas analysis and blood cell count [median (IQR)]. **Table S3** Evaluation of the stability of the whole blood model of bacteremia by analyzing neutrophil surface markers and humoral markers of inflammation [median (IQR)]. **Table S4** Characteristics of the sepsis cohort (*n*=14).
Additional file 2. Representative measurement data from a patient with sepsis with or without stimulation for the classic and the simple cellular response capacity after compensation, including the corresponding compensation matrix.
Additional file 3. Representative compensation matrices of the classic cellular response capacity from the patients with sepsis cohort.
Additional file 4. Full data set of the marker evaluation of the sepsis cohort for the cellular response capacity (CRC).

Acknowledgments

The authors acknowledge Ms. Carina Rampp and Ms. Ulrike Simnacher for skillful technical assistance.

Authors' contributions

DACM and MHL conceptualized the study, administered the project, acquired the funding, provided the resources, and wrote the original draft of the manuscript. DACM, PM, LW, FrM, LS, and RT were responsible for data curation. DACM, PM, LW, FrM, LS, AOKM, SL, RT, LS, and FiM performed the formal analysis. All authors contributed to the investigation. All authors contributed to the development of the methodology. DACM, PM, LW, BDT, FrM, and FiM prepared the visualizations. All authors contributed to the writing, review, and editing of the manuscript. All authors read and approved the final report and made the decision to submit for publication.

Funding

This work was supported by a "Gerok Rotation" (rotation as clinician scientist) to DACM, a personal grant to DACM (545061513), and project A01 (251293561) to MHL by the Collaborative Research Center 1149 (251293561), all awarded by the German Research Foundation.

Availability of data and materials

The original contributions presented in this study are included in the article/supplementary material; further inquiries can be directed to the corresponding author.

Declarations

Ethics approval and consent to participate

All experiments were conducted in accordance with the ethical standards of the Declaration of Helsinki and approved by the Local Independent Ethics Committee of the Ulm University (#319/20 and #452/21). Patients and healthy volunteers provided informed written consent before participation in the study. Further details are given in the corresponding method section.

Consent for publication

All data derived from patients or material from patients or healthy human volunteers were analysed after obtaining written informed consent from the individuals, which included the consent to publish the results.

Competing interests

The authors declare that they have no competing interests.

Author details

[1]Institute of Clinical and Experimental Trauma Immunology, University Hospital Ulm, 89081 Ulm, Germany. [2]Institute of Medical Microbiology and Hygiene, University Hospital Ulm, 89081 Ulm, Germany. [3]Institute for Transfusion Medicine, University Hospital Ulm, 89081 Ulm, Germany. [4]Clinic for Cardiothoracic and Vascular Surgery, University Hospital Ulm, 89081 Ulm, Germany. [5]Clinic for Anesthesiology and Intensive Care Medicine, University Hospital Ulm, 89081 Ulm, Germany. [6]Anesthesiology and Operative Intensive Care, Faculty of Medicine, University of Augsburg, 86156 Augsburg, Germany.

References

1. Singer M, Deutschman CS, Seymour CW, Shankar-Hari M, Annane D, Bauer M, *et al*. The third international consensus definitions for sepsis and septic shock (Sepsis-3). JAMA. 2016;315:801.
2. Fisher R, Colombo CJ, Mount CA, Mann-Salinas EA, Bostick AW, Davis K, *et al*. Critical care in the military health system: a 24-h point prevalence study. Mil Med. 2018;183:e478-85.
3. Tedesco DJ, Hutter MF, Khalaf F, Ricciuti Z, Jeschke MG. Sepsis in burn care: incidence and outcomes. Mil Med Res. 2025;12(1):55.
4. Rudd KE, Johnson SC, Agesa KM, Shackelford KA, Tsoi D, Kievlan DR, *et al*. Global, regional, and national sepsis incidence and mortality, 1990–2017: analysis for the Global Burden of Disease Study. Lancet. 2020;395:200-11.
5. Geringer MR, Stewart L, Shaikh F, Carson ML, Lu D, Cancio LC, *et al*. Epidemiology and timing of infectious complications from battlefield-related burn injuries. Burns. 2024;50:107200.
6. McCarthy SL, Stewart L, Shaikh F, Murray CK, Tribble DR, Blyth DM. Prognostic value of sequential organ failure assessment (SOFA) score in critically-ill combat-injured patients. J Intensive Care Med. 2022;37:1426-34.
7. Thompson KB, Krispinsky LT, Stark RJ. Late immune consequences of combat trauma: a review of trauma-related immune dysfunction and potential therapies. Mil Med Res. 2019;6:11.
8. Kumar A, Roberts D, Wood KE, Light B, Parrillo JE, Sharma S, *et al*. Duration of hypotension before initiation of effective antimicrobial therapy is the critical determinant of survival in human septic shock. Crit Care Med. 2006;34:1589-96.
9. Rhodes A, Evans LE, Alhazzani W, Levy MM, Antonelli M, Ferrer R, *et al*. Surviving sepsis campaign: international guidelines for management of sepsis and septic shock. Crit Care Med. 2017;45:486-552.
10. Martin GS, Mannino DM, Eaton S, Moss M. The epidemiology of sepsis in the United States from 1979 through 2000. N Engl J Med. 2003;348:1546-54.
11. Vincent JL. International study of the prevalence and outcomes of infection in intensive care units. JAMA. 2009;302:2323.
12. Huber-Lang M, Lambris JD, Ward PA. Innate immune responses to trauma. Nat Immunol. 2018;19:327-41.
13. Kolaczkowska E, Kubes P. Neutrophil recruitment and function in health and inflammation. Nat Rev Immunol. 2013;13:159-75.
14. Hotchkiss RS, Moldawer LL, Opal SM, Reinhart K, Turnbull IR, Vincent JL. Sepsis and septic shock. Nat Rev Dis Primers. 2016;2:16045.
15. Messerer DAC, Schmidt H, Frick M, Huber-Lang M. Ion and water transport in neutrophil granulocytes and its impairment during sepsis. Int J Mol Sci. 2021;22:1699.
16. Chen L, Zhang X, Shi P. Recent advances in biomarkers for detection and diagnosis of sepsis and organ dysfunction: a comprehensive review. Eur J Med Res. 2025;30:1081.
17. Hashem HE, Ahmed WO, Hassan SH. The role of neutrophil CD11b compared to neutrophil CD64 as an early diagnostic, monitoring, and prognostic sepsis marker in neonatal ICUs: case-control-methodological study. Biomed Res Int. 2025;2025:7206112.
18. Gong T, Liu YT, Fan J. Exosomal mediators in sepsis and inflammatory organ injury: unraveling the role of exosomes in intercellular crosstalk and organ dysfunction. Mil Med Res. 2024;11(1):24.
19. Papareddy P, Selle M, Partouche N, Legros V, Rieu B, Olinder J, *et al*. Identifying biomarkers deciphering sepsis from trauma-induced sterile inflammation and trauma-induced sepsis. Front Immunol. 2024;14:1310271.
20. Pepys MB, Hirschfield GM. C-reactive protein: a critical update. J Clin Invest. 2003;111:1805-12.
21. Wacker C, Prkno A, Brunkhorst FM, Schlattmann P. Procalcitonin as a diagnostic marker for sepsis: a systematic review and meta-analysis. Lancet Infect Dis. 2013;13:426-35.
22. Gelbard RB, Hensman H, Schobel S, Stempora LL, Moris D, Dente CJ, *et al*. An integrative model using flow cytometry identifies nosocomial infection after trauma. J Trauma Acute Care Surg. 2021;91:47-53.
23. Yao R, Li Z, Wang L, Li Y, Zheng L, Dong N, *et al*. Single-cell transcriptome profiling of the immune space-time landscape reveals dendritic cell regulatory program in polymicrobial sepsis. Theranostics. 2022;12:4606-28.
24. Chen G, Chong H, Zhang P, Wen D, Du J, Gao C, *et al*. An integrative model with HLA-DR, CD64, and PD-1 for the diagnostic and prognostic evaluation of sepsis. Immun Inflamm Dis. 2024;12:e1138.
25. Pillay J, Kamp VM, van Hoffen E, Visser T, Tak T, Lammers JW, *et al*. A subset of neutrophils in human systemic inflammation inhibits T cell responses through Mac-1. J Clin Invest. 2012;122:327-36.
26. Shankar-Hari M, Datta D, Wilson J, Assi V, Stephen J, Weir CJ, *et al*. Early prediction of sepsis using leukocyte surface biomarkers: the ExPRES-sepsis cohort study. Intensive Care Med. 2018;44:1836-48.
27. Yeh CF, Wu CC, Liu SH, Chen KF. Comparison of the accuracy of neutrophil CD64, procalcitonin, and C-reactive protein for sepsis identification: a systematic review and meta-analysis. Ann Intensive Care. 2019;9:5.
28. Bernhard S, Hug S, Stratmann AEP, Erber M, Vidoni L, Knapp CL, *et al*. Interleukin 8 elicits rapid physiological changes in neutrophils

that are altered by inflammatory conditions. J Innate Immun. 2021;13:225-41.
29. Hug S, Bernhard S, Stratmann AEP, Erber M, Wohlgemuth L, Knapp CL, *et al*. Activation of neutrophil granulocytes by platelet-activating factor is impaired during experimental sepsis. Front Immunol. 2021;12:642867.
30. Messerer DAC, Vidoni L, Erber M, Stratmann AEP, Bauer JM, Braun CK, *et al*. Animal-free human whole blood sepsis model to study changes in innate immunity. Front Immunol. 2020;11:571992.
31. Stratmann AEP, Wohlgemuth L, Erber ME, Bernhard S, Hug S, Fauler M, *et al*. Simultaneous measurement of changes in neutrophil granulocyte membrane potential, intracellular pH, and cell size by multiparametric flow cytometry. Biomedicines. 2021;9:1504.
32. Jovanovski D, Wohlgemuth L, Lessing PML, Hüsken D, Koller AS, Thomaß BD, *et al*. Multimodal monitoring of neutrophil activity during cardiac surgery. Front Immunol. 2025;16:1504944.
33. Connelly AN, Huijbregts RPH, Pal HC, Kuznetsova V, Davis MD, Ong KL, *et al*. Optimization of methods for the accurate characterization of whole blood neutrophils. Sci Rep. 2022;12:3667.
34. Wohlgemuth L, Stratmann AEP, Münnich F, Bernhard S, Thomaß BD, Münnich F, *et al*. Modulation of neutrophil activity by soluble complement cleavage products – an in-depth analysis. Cells. 2022;11:3297.
35. Kumar R, Kattimani B, Ojha PR, Khasage UJ. Quick sequential organ failure assessment score, lactate, and neutrophil-lymphocyte ratio help in diagnosis and mortality prediction during golden hour of sepsis in emergency department. J Emerg Trauma Shock. 2023;16:161-6.
36. He RR, Yue GL, Dong ML, Wang JQ, Cheng C. Sepsis biomarkers: advancements and clinical applications – a narrative review. Int J Mol Sci. 2024;25:9010.
37. Eppensteiner J, Kwun J, Scheuermann U, Barbas A, Limkakeng AT, Kuchibhatla M, *et al*. Damage- and pathogen-associated molecular patterns play differential roles in late mortality after critical illness. JCI Insight. 2019;4:e127925.
38. Qiu X, Li J, Yang X, Tang J, Shi J, Tong Y, *et al*. Is neutrophil CD11b a special marker for the early diagnosis of sepsis in neonates? A systematic review and meta-analysis. BMJ Open. 2019;9:e025222.
39. Weirich E, Rabin RL, Maldonado Y, Benitz W, Modler S, Herzenberg LA, *et al*. Neutrophil CD11b expression as a diagnostic marker for early-onset neonatal infection. J Pediatr. 1998;132:445-51.
40. Maecker HT, McCoy JP, Nussenblatt R. Standardizing immunophenotyping for the Human Immunology Project. Nat Rev Immunol. 2012;12:191-200.
41. Choudhary T, Upadhyaya P, Davis CM, Yang P, Tallowin S, Lisboa FA, *et al*. Derivation and validation of generalized sepsis-induced acute respiratory failure phenotypes among critically ill patients: a retrospective study. Crit Care. 2024;28:321.
42. Yang B, Wang X, Liu Z, Lu Z, Fang G, Xue X, *et al*. Endothelial-related biomarkers in evaluation of vascular function during progression of sepsis after severe trauma: new potential diagnostic tools in sepsis. J Inflamm Res. 2023;16:2773-82.
43. Yadgarov MY, Landoni G, Berikashvili LB, Polyakov PA, Kadantseva KK, Smirnova AV, *et al*. Early detection of sepsis using machine learning algorithms: a systematic review and network meta-analysis. Front Med. 2024;11:1491358.
44. Tobin JM, Gavitt BJ, Nomellini V, Dobson GP, Letson HL, Shackelford SA. Immunotherapeutic options for inflammation in trauma. J Trauma Acute Care Surg. 2020;89:S77-82.

https://doi.org/10.1016/j.mmr.2026.100010
Cite this article as: Messerer DAC, Müller P, Wohlgemuth L, Münnich F, Stukan L, Mohamed AOK, *et al*. The cellular response capacity (CRC) as a novel immunomonitoring approach in sepsis. *Mil Med Res*. 2026;13(1):100010.